International
Progress Report

IPR-08-06

Äspö Hard Rock Laboratory

Prototype Repository

Inverse modelling of a Prototype Repository using near-field groundwater samples from July 1998 – March 2004

Ari Luukkonen

VTT

February 2008

Svensk Kärnbränslehantering AB
Swedish Nuclear Fuel
and Waste Management Co

Box 250, SE-101 24 Stockholm
Phone +46 8 459 84 00

Äspö Hard Rock
Laboratory

Report no.	No.
IPR-08-06	F63K
Author	Date
Ari Luukkonen	2008-02-28
Checked by	Date
Teresita Morales Ignasi Puigdomenech	March 2008
Approved	Date
Anders Sjöland	2008-04-15

Äspö Hard Rock Laboratory

Prototype Repository

Inverse modelling of a Prototype Repository using near-field groundwater samples from July 1998 – March 2004

Ari Luukkonen

VTT

February 2008

Keywords: Äspö HRL, Prototype Repository, Hydrogeochemistry, Inverse modelling, Mixing, Mass transfer

Abstract

A full-scale final repository experiment, in accordance with the KBS-3V concept, is in progress at the Äspö Hard Rock Laboratory, Sweden. This prototype repository is heavily instrumented with sensors and instruments to monitor the repository interior and its near field. The repository includes six deposition holes, 8 metres deep and 1.75 metres in diameter. The repository tunnel is located 450 metres below ground level, and is about 63 metres long and 5 metres in diameter. Each deposition hole contains a full-sized canister and each canister is equipped with an electric heating device to simulate the production of heat by radioactive decay in the real repository. It is planned to monitor the prototype repository for about 20 years. However, parts of the repository may be dismantled within a few years.

Groundwater was sampled at several locations in the near-field bedrock over six years. The results of geochemical analysis are interpreted with an inverse modelling approach implemented within the PHREEQC-2 hydrogeochemical modelling code. The main purpose of this inverse modelling was to estimate mixing fractions of the reference water types in the samples. The reference water types were interpreted from the geological history of the area. Calculations of mass transfer also indicate the extent of geochemical reactions needed to reproduce individual samples. The analytical uncertainties were taken into account in the calculations. This makes the results of the calculation more robust in general, and also gives numerical estimates of the reliability of the results.

The results of the inverse modelling calculations indicate that the major sources of water infiltrating the near field of the prototype repository are from above. The most significant source is the Baltic Sea, the second largest source is the remnant ancient seawater reserves within the bedrock, while the third notable source is of meteoric origin. Only slight changes in mixing fractions and water compositions as a function of time were detected. Calculations of the cumulative total mass transfer for the near-field samples indicate that mineral reactions related to carbonate and sulphur equilibria, and cation-exchange processes have occurred along the pathways from the sources to the sampling points. Approximate values of total mass transfer based on actual samples can provide useful information. For example, regional-scale forward modelling for the prediction of future evolution could be calibrated against current knowledge regarding hydrological flow and geochemical mass transfer, thus improving the reliability of predictions.

As part of the current study, a small set of baseline samples, collected around Äspö prior to the Hard Rock Laboratory excavations, were utilised in the inverse calculations. The results obtained using these samples indicate that characteristic mass transfer related to the Äspö glaciation and postglacial stages has occurred in the bedrock.

Sammanfattning

Ett fullskaligt slutförvarsexperiment enligt KBS-3V-konceptet pågår vid svenska Äspölaboratoriet. Detta prototypförvar är försett med ett stort antal sensorer och instrument för övervakning av förvarets inre delar och dess närområde. Förvaret omfattar sex deponeringshål, 8 meter djupa och 1,75 meter i diameter. Tunneln där försöket äger rum är belägen 450 meter under marknivån. Den är cirka 63 meter lång och 5 meter i diameter. Varje deponeringshål innehåller en kapsel i fullstorlek, och varje kapsel är försedd med en elektrisk värmare som simulerar värmeproduktionen från radioaktivt sönderfall i ett verkligt förvar. Man planerar att övervaka prototypförvaret i ungefär 20 år. Delar av förvaret kan emellertid komma att demonteras inom några år.

Grundvattenprover har tagits på ett flertal platser i den intilliggande berggrunden under sex år. Resultaten från den geokemiska analysen tolkades med en inversmodelleringsmetod som ar inkluderad i hydrogeokemisk modellering koden PHREEQC-2. Det främsta syftet med denna inversmodellering var att uppskatta blandningsproportionerna för referensvattentyperna i proverna. Referensvattentypernas sammansättning valdes med utgångspunkt i områdets geologiska historia. Med masstransportberäkningar kan man även påvisa den nödvändiga omfattningen av geokemiska reaktioner för att reproducera individuella prover. Vid beräkningarna har man tagit hänsyn till osäkerheterna i analyserna. Detta har gjort att beräkningsresultaten generellt blivit mer robusta och att deras pålitlighet har kunnat uppskattas numeriskt.

Resultaten från inversmodelleringen tyder på att det mesta av det vatten som infiltrerar prototypförvarets närområde kommer ovanifrån. Den mest betydande källan är Östersjön, den näst största källan utgörs av gammalt havsvatten i berggrunden medan den tredje noterbara källan är av meteroiskt ursprung. Man fann endast mindre förändringar i blandningsproportioner och vattensammansättningar som en funktion av tiden. Beräkningar av den kumulativa totala masstransporten för proverna från närområdet tyder på att mineralreaktioner relaterade till karbonat- och svaveljämvikter samt katjonbytesprocesser har ägt rum längs vägen från källorna till provtagningsställena. Ungefärliga värden på den sammanlagda masstransporten, baserat på verkliga prover, kan ge användbar information. Exempelvis kan framåtmodellering i regional skala för förutsägelser om den framtida utvecklingen kalibreras mot aktuell kunskap om hydrologiska flöden och geokemisk masstransport, vilket kan förbättra säkerheten i förutsägelserna.

Som en del i den aktuella studien användes en mindre uppsättning prover, insamlade på Äspö före utgrävningarna för laboratoriebygget, som utgångslägesreferens i de inversa beräkningarna. Resultaten som erhölls med dessa prover visar att en karaktäristisk masstransport härrörande från glaciala och postglaciala skeenden på Äspö har ägt rum i berggrunden.

Contents

Notation

Abbreviations

$\delta^{18}O$ Accepted unit of $^{18}O/^{16}O$ ratio given in per mill (‰) and calculated from Standard Mean Ocean Water (SMOW) as follows:

$$\delta^{18}O_{Sample} = \frac{\left(^{18}O/_{16}O\right)_{Sample} - \left(^{18}O/_{16}O\right)_{SMOW}}{\left(^{18}O/_{16}O\right)_{SMOW}} \cdot 1000$$

CRT Canister retrieval test

HASxxx Percussion borehole started from ground surface

HRL Hard rock laboratory

KASxxx Core drilled borehole started from ground surface

KBS-3V Nuclear waste disposal concept where spent fuel assemblies are sealed in copper-iron canisters and are emplaced in vertical deposition holes of a repository excavated at a depth of about 500 metres in crystalline bedrock

LTDE Low temperature diffusion experiment

REX Redox experiment

SICADA SKB's Site characterisation database

TRUE Tracer retention understanding experiment

ZEDEX A study of the zone of excavation disturbance from tunnel excavation

General data

Laxemar Swedish candidate site for final repository of nuclear waste located 2 km SW from the Äspö Island

1 Introduction

A full-scale experiment simulating a final repository for high-level nuclear waste is in progress at Äspö Hard Rock Laboratory (HRL), north of Oskarshamn, south-eastern Sweden. This prototype repository experiment has been designed in accordance with the KBS-3V concept where spent nuclear fuel assemblies are emplaced in copper-iron canisters in a repository excavated at a depth of about 500 metres in the crystalline bedrock. Moreover, the prototype repository is heavily instrumented with sensors and instruments to measure the thermal, hydrological, mechanical and geochemical evolution of the experimental system (Pusch & Börgesson 2001, Puigdomenech & Sandén 2001, Barcena & Garcia-Sineriz 2001, Börgesson & Sandén 2003, Rhén et al. 2001, 2003). In the prototype repository experiment full-sized canisters, placed in deposition holes, are equipped with electric heaters to simulate the heat produced by spent radioactive fuel in a future repository.

The prototype repository consists of a tunnel approximately 63 metres long, excavated with a tunnel boring machine 450 metres below ground level (Fig. 1-1). The experimental repository includes six vertical, bentonite-buffered deposition holes, a backfilled tunnel, and two concrete plugs that divide the prototype tunnel into two sections (Fig. 1-2). Both the deposition holes and the tunnel sections are extensively instrumented and regularly or frequently monitored. The diameter of the prototype tunnel is 5 metres. The canister deposition holes are 8 metres deep and 1.75 metres in diameter. The distance between deposition holes within the sections (Sections 1 and 2) is approximately 6 metres.

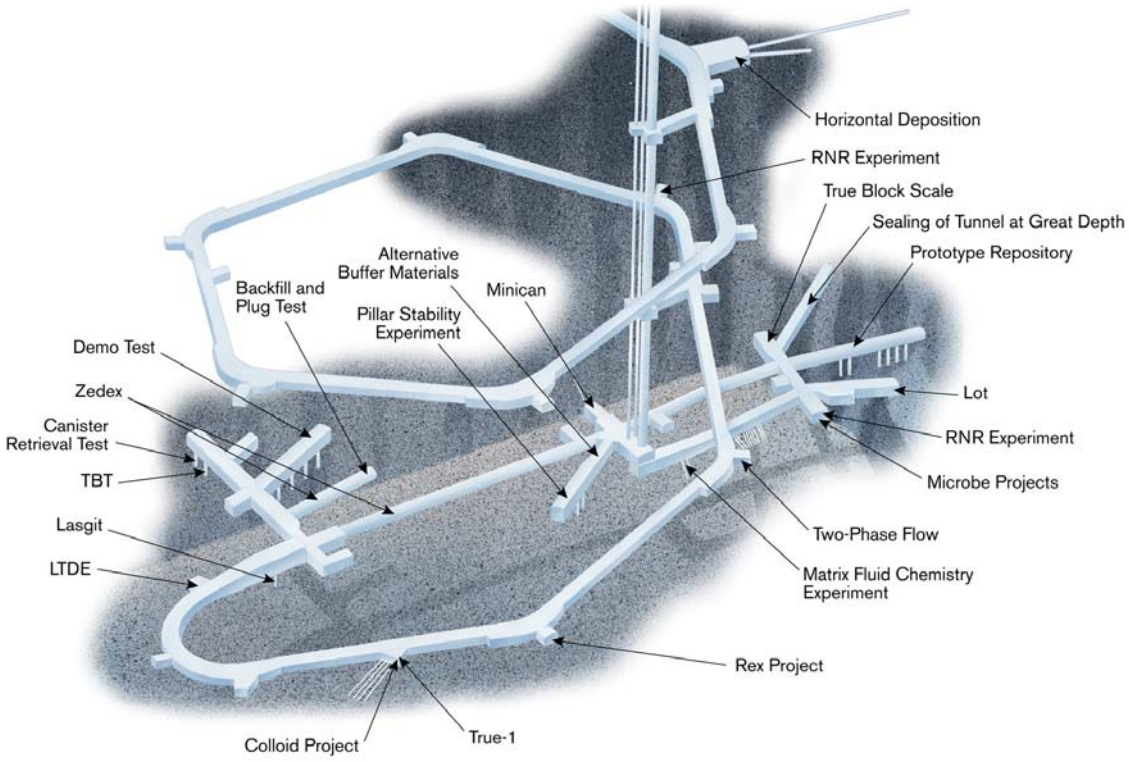

Figure 1-1. *Schematic view showing the location of the prototype repository at the Äspö Hard Rock Laboratory (SKB 2007).*

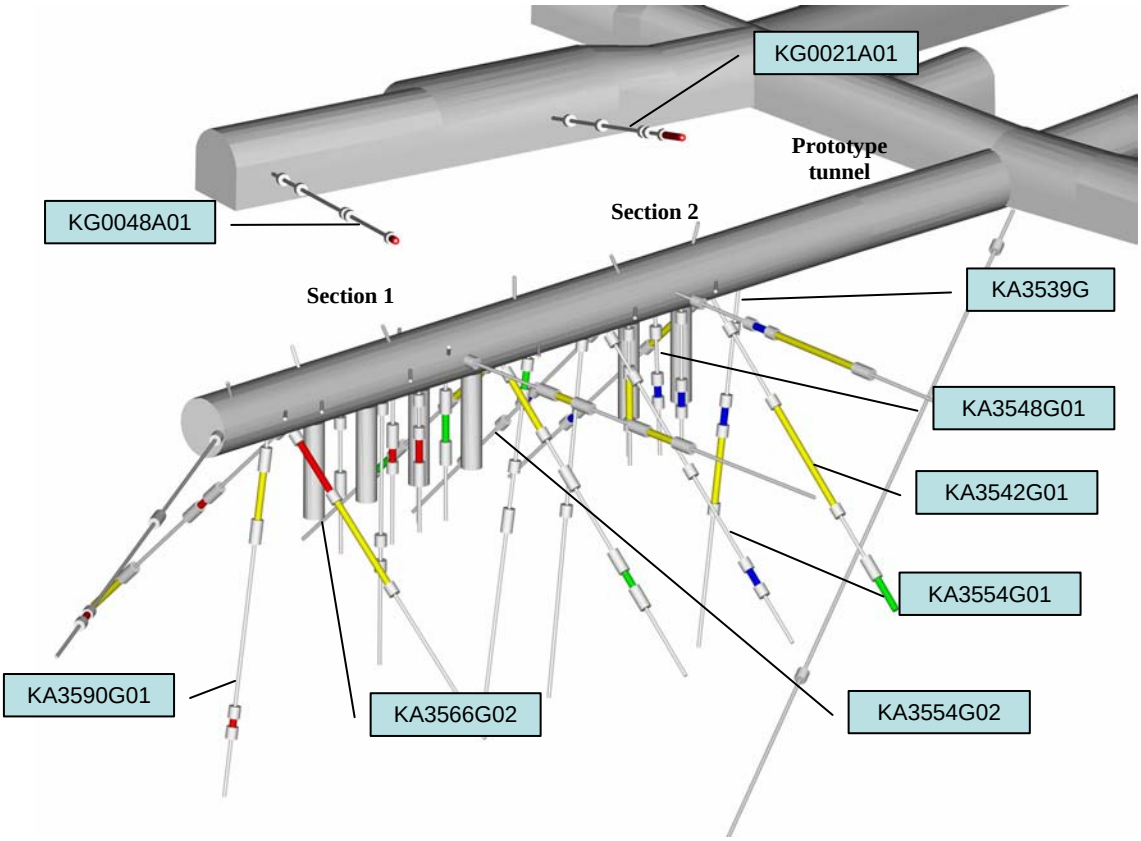

Figure 1-2. *Locations of sampled near-field boreholes in this work (modified after Rhén et al. 2003).*

It is intended to monitor the prototype repository for up to 20 years. However, section 2 may be dismantled within few years. During the construction of the repository, state-of-the-art knowledge was gained on emplacement techniques, backfilling and sealing. It was possible, for the first time, to simulate the disposal of canisters with the size and weight of real canisters in vertical boreholes, in accordance with the KBS-3V concept. The experiment is expected to provide information on the long-term performance of this repository concept. Many processes are being studied (SKB 2005).

- Water uptake in buffer and backfill
- Temperature distribution in canisters, buffer, backfill and rock
- Displacement of canisters
- Swelling pressure and displacement in buffer and backfill
- Stresses and displacement in the near-field rock
- Water pressure build-up and pressure distribution in rock
- Gas pressure in buffer and backfill
- Chemical processes in rock, buffer and backfill
- Bacterial growth and migration in buffer and backfill

1.1 Geochemical modelling

The results presented in this report concern groundwater composition and geochemical processes in the bedrock surrounding the repository tunnel. The locations of the near-field boreholes sampled in this study are shown in Figure 1-2. In addition to the samples collected around the prototype repository tunnel, geochemical data from groundwater on the island of Äspö prior to the Äspö HRL excavations have also been used. These data are referred to as Äspö baseline samples and they are believed to represent undisturbed hydrogeochemical conditions on the island.

The interpretation of geochemical data is based on the inverse modelling approach, first introduced by Plummer, Parkhurst and Thorstenson in 1983 (Plummer et al. 1983). In inverse modelling, geochemically conservative species (i.e. practically inert species in low temperature saturated hydrogeochemical systems), such as e.g. Cl and stable light isotopes such as $\delta^{18}O$, have a significant effect on the interpretation of the analytical results obtained from groundwater samples. The conservative species define how a set of initial water types are mixed with each other. All the other species included in the calculations (e.g. Na, Ca, SO_4, etc.) are subject to mass transfer (i.e. chemical reactions). The objective of the current study was to determine how the composition of the groundwater samples arose from the mixture of a set of reference water types. These reference water types represent different water sources, which can be either modern (meteoric, Baltic Sea) or relict (e.g. Littorina Sea, Pleistocene glacial meltwater).

Inverse modelling has been applied to variety of hydrogeochemical problems. It is perhaps most common in environmental remediation studies (e.g. Desbarats & Dirom 2007, Eary et al. 2003).

The strength of the inverse method is that quantitative estimates of the mixing ratios and mass transfer are obtained. Analytical revision of the results of the calculations is part of the process, and includes the critical review of calculated mixing ratios, the amount of mass transfer and, importantly, also the direction of mass transfer. The resulting mixing ratios contribute to the historical evolution of the samples. In the final results, the amount and direction of mass transfer should be realistic bearing in mind the evolution history.

The consistency between the hydrogeological evolution at a site, and the sources deduced from the water sampled from the site indicates how well the model has performed. Consistency considerations can be applied to the early history of the site or confined to short time spans if relatively rapid changes occur in the hydrogeological system. In the current study, the short-term considerations are of primary concern. Inverse hydrogeochemical interpretation of water samples indicates the major sources of the groundwater surrounding the prototype repository. Assumptions can be made regarding the fracture systems and their effects on the water sources, e.g. on hydraulic conductivity and zone geometry, and on the channelling of the groundwater flow within fracture zones. However, hydrogeological considerations are not the subject of interest in the current study. Only the hydrogeochemistry of a series of samples is considered, and the emphasis is placed on defining the water sources and the processes taking place during water transport.

2 THE Inverse-modelling approach

2.1 General aspects

The inverse-modelling method is a combination of speciation modelling and mass-balance modelling. Speciation modelling, petrographic observations, the reactions expected to dominate in a groundwater system, and isotopic data provide the constraints for inverse studies. In accordance with these constraints, mass-transfer modelling provides quantitative net reactions that reproduce the compositions of the samples and are consistent with any constraints on the reactant phase (see e.g. Parkhurst & Plummer 1993, Runnells 1993). The processes of dissolution and precipitation of minerals, gases, and organic matter, in addition to ion exchange and oxidation/reduction processes, can be represented by the following mass-transfer formula:

Initial water compositions + "reactant phases" → final water composition + "product phases" 2-1

The modelling tool used in this study was PHREEQC-2 (Parkhurst & Appelo 1999). PHREEQC-2 handles the normal inverse-modelling routines and it has the capability for inverse modelling within specified chemical and isotopic compositional uncertainties. Taking analytical uncertainties into account PHREEQC-2 provides simpler and more robust mass-transfer models than calculations without uncertainties. The utilisation of uncertainties also allows the evaluation of the significance of mixing fractions and mass transfer (Parkhurst 1997).

2.2 Calculation constraints

2.2.1 Reacting phases

The geochemical mass-transfer reactions considered in this study are the dissolution/precipitation of calcite, dissolution of dolomite, consumption of organic matter (CH_2O), dissolution of goethite, precipitation of pyrite, and the ion-exchange processes between Na, K, Ca, Mg and Fe. Table 2-1 lists the solid phases included in the calculations.

Table 2-1. Selected solid phases for mass-balance modelling and their compositions. Source (+) and sink (-) terms indicate release and retardation of elements into phases.

Phase	Source(+)/Sink(-)	Composition
Calcite	+/-	$CaCO_3$
Dolomite	+	$CaMg(CO_3)_2$
Organic matter	+	CH_2O
Goethite	+	FeOOH
Pyrite	-	FeS_2
Cation exchange	+/-	NaX, CaX_2, KX, MgX_2, FeX_2

Reactions such as the dissolution of CO_2 (organic respiration) and O_2 (atmospheric), related mainly to the unsaturated soil layer above the bedrock, were not included in the calculations. The meteoric reference water used in the calculations was chosen such that these reactions have already modified the reference water composition.

The ion-exchange processes related to Na, K, Ca, Mg and Fe were not defined in detail. Other reacting species, in addition to normal carbonate and exchange processes, are montmorillonite, kaolinite and chlorite, which are common alteration products of feldspars and biotite (Andersson 1996). These mineral species were not included in the inverse calculations, although aqueous concentrations of silica (SiO_2) in samples are given.

The anaerobic production and consumption of CH_4 (methanogenesis and anaerobic methane oxidation) were not considered in the current study. According to the theoretical redox sequence, methane-containing groundwater is usually low in sulphate-containing minerals (Appelo & Postma 1993, 2005). However, all deep Äspö groundwater samples are rich in SO_4. In principle, methane consumption (oxidation) coupled with sulphate reduction is a possible process at the Äspö site.

2.2.2 Analytical data

From the stored SKB database values (SICADA) of pH, Na, K, Ca, Mg, Fe_{tot}, HCO_3, Cl, SO_4 and $\delta^{18}O$ for each sample were used for modelling. In the inverse calculations, Cl and ^{18}O concentrations were considered as conservative parameters, i.e. these two parameters essentially define the mixing fractions between two or three initial water samples (cf. Equation 2-1).

The uncertainty in the analytical results for Na, Ca, Mg and HCO_3 was defined to be 4%; that for Cl 5%, for SO_4 and K 6%, and for Fe 10%. The uncertainties in pH and $\delta^{18}O$ were set to 0.04 and 0.2 units, respectively. The dissolved SO_4 level in two baseline samples (KAS06/-433.3 and KAS03/-830.1, cf. Table 3-1) was so high that these waters could not be reproduced from the baseline samples without exceeding the uncertainty constraint. The uncertainty in SO_4 for these two samples was thus set to 20%. All other uncertainty levels were as given above.

2.2.3 Reference water types

A detailed study of the geochemical data from the Äspö site requires an interpretation of the palaeohydrology of the area. Based on published conceptual models of the evolution of the Äspö area (e.g. SKB 2006), and on the interpretations of the geochemical data, a simplified history of the Äspö site was constructed (Fig. 2-1). The Quaternary history of the area was divided into four main, hydrogeochemically significant, stages that cover the present, Littorina Sea, glacial and preglacial ages. Specific reference water types have infiltrated the bedrock during each of these periods.

The recent water types (Fig. 2-1d) considered here are recharging meteoric water and seawater recharging the bedrock from the present Baltic Sea. The compositions of the meteoric and seawater reference water types are given in Table 2-1.

The meteoric reference water type has been sampled from the centre of the undisturbed island of Äspö and its composition has been reported (Laaksoharju 1988). According to Laaksoharju water from the location HAS05/-56.3m is representative of a Na-HCO_3, non-saline, dilute granitic water that has acquired sodium and bicarbonate from surficial weathering of plagioclase and calcite, respectively. However, organic respiration in the unsaturated zone has also contributed to the HCO_3 content. In the baseline analytical data used here, the sample HAS05/-56.3m represents the most dilute bedrock groundwater sample (Cl = 119 mg/L) on the island of Äspö. The HAS05/-56.3m sample has a relatively high SO_4 content (SO_4 = 118 mg/L) for water originating from a meteoric source.

The seawater reference used is an average of six samples taken from the Baltic during the summers of 1992 and 1993 off the coast of Äspö. Sample IDs and dates are given in Table 2-1. The average used is somewhat less saline than the previously used Baltic Sea reference (cf. Laaksoharju & Wallin 1997, p. 32), indicating dilution of coastal Baltic seawater as a consequence of recharging of surficial fresh water from land areas.

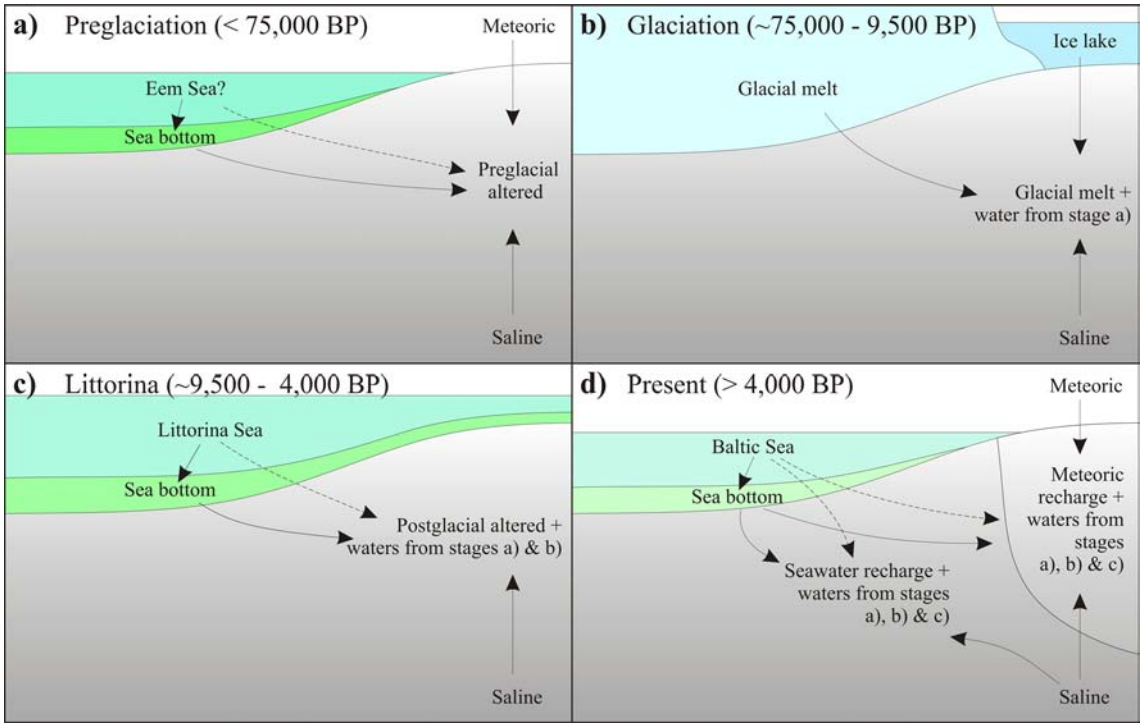

Figure 2-1. *Simplified Quaternary history of the Äspö area. The interpretation is based on the analysis of geochemical data and on the interpretation of the Quaternary history of the Äspö area (e.g. Laaksoharju & Wallin 1997, SKB 2006). Only periods deemed to have a significant effect on groundwater evolution at the Äspö site are considered.*

Table 2-1. Reference water types used in the inverse-modelling calculations. Meteoric, postglacial altered and saline reference water types are actual baseline samples.

	Meteoric water [a)]	Baltic Sea [b)]	Postglacial altered [c)]	Littorina Sea [d)]	Glacial melt [e)]	Preglacial altered [f)]	Saline [g)]
pH	8.0	7.7	7.3	7.6	5.8	7.7	8.0
Na	237	1904	1880	3764	0.2	1700	3020
K	4.0	72.7	32.8	134	0.2	(4.0)	7.3
Ca	25.0	90.9	1040	151	0.1	450.0	4380
Mg	6.0	226	219	448	0.1	110.0	49.5
Alkalinity	370	85.7	132	92.5	0.2	200	11.0
Cl	119	3562	5070	6500	0.7	3500	12300
SO_4	118	505	136	890	0.1	100	709
Si	5.2	0.3	5.0	1.8	0.0	(4.7)	4.2
Fe	1.6	0.08	2.7	0.002	0.0	1.7	0.08
$\delta^{18}O$	-9.9	-6.4	-7.2	-4.7	-19.0	-9.5	-12.7

a) HAS05/-56.3m (Aug. 7, 1987).

b) Average of 6 samples PASSEA01 (Aug. 28,1992) & PASSEA01-05 (Aug. 7, 1993)

c) HAS13/-42.0m (July 3, 1989).

d) From Andersson et al. (2007) & refs. therein

e) From Andersson et al. (2007) & refs. therein with reconsidered $\delta^{18}O$ value

f) From Luukkonen & Kattilakoski (2001)

g) KAS03/-914.1m (March 15, 1989).

The Littorina stage (Fig. 2-1c), starting at about 9,500 BP and preceding the present stage, can be clearly identified from the hydrogeochemical data. Samples significantly contaminated by *postglacial altered* marine water are characterised by higher salinities than the present Baltic Sea and high $\delta^{18}O$ values. According to the interpretations, the postglacial altered marine waters originated from seawater related to the Littorina Sea stage.

Based on the studies of groundwater salinity, past temperature, and subfossil shells discovered in the region of Hästholmen, Finland, Kankainen (1986) proposed that $\delta^{18}O$ and Cl values in the Littorina Sea were probably initially -4.7‰ and 6,500 mg/L, respectively. There are, however, also certain fossil indications that, at least in the southern part of the Littorina Sea, water has been significantly more saline than indicated by the Cl values presented in Table 2-1 (cf. Laaksoharju & Wallin 1997, p. 34). The other main elemental concentrations presented in Table 2-1 are the result of dilution of the estimated global mean ocean water (see Andersson et al. 2007 for details).

Although, the *postglacial altered* water type is considered together with the Littorina Sea reference water, no strict time span for formation of postglacial altered water can be assigned. The postglacial altered water type is representative of seawater that has infiltrated the sea bottom sediments (Fig. 2-1c). During infiltration, extensive reduction of aqueous sulphate driven by organic activity, coupled with multiple recycled

oxidation-reduction reactions of iron take place (cf. Canfield et al. 1993, Wang & Van Chappellen 1996). Similarly, significant complex cation-exchange processes occur in the sea bottom, causing the depletion of Na and Mg, and enrichment of Ca in the recharging water. The postglacial altered reference water composition used (HAS13/-42.0m) is given in Table 2-1. Its Cl content is less than estimated for the Littorina Sea reference, but clearly higher than that in the present Baltic Sea (cf. Fig. 2-3). Therefore, the formation of postglacial altered water cannot not to be restricted to the early (saline) period of the Littorina Sea stage. Since the start of the Littorina Sea stage, seawater has gradually become diluted to the present seawater salinity. The Littorina stage lasted until 2,500–2,000 BP. However, significant seawater influence ceased when the island of Äspö rose above sea level, about 4,000 years ago (SKB 2006).

During *the glacial stage* (Fig. 2-1b), meltwater from the Pleistocene ice sheet is considered to be the dominant source of water recharging the bedrock. Glacial meltwater is very dilute and poorly buffered. The main uncertainty lies in the average value of $\delta^{18}O$. Laaksoharju & Wallin (1997) and Pitkänen et al. (1999, 2004) interpreted almost consistently that glacial meltwater had an average $\delta^{18}O$ value of -20‰ to -22‰. Studies on ice sheets on Greenland (e.g. Taylor et al. 1992) indicate distinctly lower $\delta^{18}O$ values for ice (-33 to -38‰). However, much of the meltwater could have recharged the bedrock during deglaciation, while the mean annual temperature rose above 0°C and rainwater diluted extreme $\delta^{18}O$ values of melting ice. In the current study, the $\delta^{18}O$ value for glacial melt was estimated to be -19‰. Other estimated concentrations for glacial meltwater are presented in Table 2-1.

The preglacial stage (Fig. 2-1a) is the oldest water-recharging period considered in the present study. The *preglacial altered* water type cannot be identified directly from Äspö groundwater and its composition (Table 2-1) is based on the Quaternary history of the Äspö region, and on argumentation of the estimated glacial melt composition (Laaksoharju & Wallin 1997, Pitkänen et al. 1999, 2004) and the most glacial type samples analysed from the Äspö Island.

Based on assumed concentrations of SO_4 and $\delta^{18}O$ in Littorina Sea water and glacial meltwater, and the current concentrations in brackish SO_4 groundwater, it was estimated that the values of $\delta^{18}O$ and Cl concentration in preglacial altered water in Olkiluoto, Finland were about -11 to -10‰ and about 3,500 mg/L, respectively (Pitkänen et al. 1999). However, similar reasoning cannot be applied at the Äspö site because it appears that a significant proportion of the infiltrated Littorina Sea water has experienced sulphate reduction (cf. postglacial altered water) during penetration through sea bottom sediments. Moreover, in the Äspö case, the altered Littorina Sea water has mixed with a body of SO_4-containing water consisting of glacial, preglacial altered and saline reference water types.

As Figure 2-1 shows, the preglacial altered water was an admixture from several preglacial sources containing contributions from at least meteoric and saline sources, and probably also from ancient seawater and altered seawater infiltrated through sea bottom sediments.

For current purposes, the Cl and ^{18}O concentrations in “preglacial altered” groundwater were estimated to be about 3,500 mg/L and -9.5‰, respectively. These estimates approximate those used in the studies at Olkiluoto, and they form the basis for estimates of other element concentrations presented in Table 2-1. The values given in the table

were calculated with the aid of three distinctly glacial-water-contaminated baseline samples (KAS03/-121.8m, KAS03/-239.0m and KAS02/-199.8m), and with one sample contaminated mainly by saline reference water (KAS02/-881.3m). Further details concerning these calculations are given by Luukkonen & Kattilakoski (2001).

For *the saline reference water* (KAS03/-914.1m) no strict age relation was assumed. The source of saline water is considered to be a large one. Saline water can be considered to be old, but diluted, water in the Äspö area. The sample KAS03/-914.1m is the most saline, $\delta^{18}O$-analysed undisturbed sample found from the island of Äspö.

2.3 Calculation method

Calculations of the mixing fractions are based on Cl and $\delta^{18}O$, which are considered conservative species in groundwater mixing. All other species taken into account are subject to mass transfer, i.e. they are transferred from/to solid reacting phases to satisfy the calculation constraints.

The inverse calculations are performed in steps assuming that the steady-state condition of chemical reactions prevails. In practice this means that a final water composition can be obtained from a realistic set of initial water samples with small, moderate or otherwise feasible mass transfer (cf. Equation 2-1). The direction of mineral reactions and the direction of cation exchange form the basis for acceptability judgement of the steady-state condition (cf. Table 2-1). Furthermore, judgements depend on which initial water samples are mixed together. For example, if a significant amount of Baltic Sea water is required, Na^+ will not be released from cation exchange but from seawater. However, if the saline reference (KAS03/-914.1m) dominates in the initial sample set, only small organic matter consumption (restricted microbial activity at depth) and small overall mass transfer between other dissolved ions may be expected, because saline water is assumed to be well-equilibrated with its environment.

The inverse-modelling approach can be said to be an iterative process based on an attempt to understand the geochemical system along a flow path. In the current approach, a previous successful (assumed steady-state) step leads to the following step, which is to find new sets of initial water samples for previous initial water samples now considered as final water samples, and so on. In many cases trial and error calculations are performed until a feasible set of mass-transfer phases and an acceptable set of initial water samples are found for a certain final water composition. The steady state steps are ultimately extended to the reference water types and then mixing fractions of the reference water types in each sample, considered in the calculation chain, can be determined. The success of inverse calculations is a function of the samples available. The more there are samples available the more there are usually feasible choices for steady state steps, and from these choices one set of initial water samples together with calculated mass transfers can be judged as a best one. Occasionally, large changes in concentration must be accepted as fulfilling the steady-state assumption. In such cases exceptional mass transfer should be avoided as far as is possible.

As an example, the concept of the calculation process is presented in Figure 2-2. Five reference water types are referred to in the figure (REF A–E) and 7 water samples (S_1-S_7). The choice of steady-state steps is based on the identification of the geochemical affinities for each sample, and finding a suitable initial water assemblage for each of the

7 samples (one or two suitable initial water samples usually exhibit similar chemical affinities to the final water). According to the example presented in Figure 2-2, following sets of water mixings can be defined for the samples.

$S_1 = 0.2*S_2 + 0.5*S_3 + 0.3*\text{REF E}$ 2-2
$S_2 = 0.1*S_3 + 0.5*S_5 + 0.4*\text{REF E}$ 2-3
$S_3 = 0.2*S_4 + 0.4*S_6 + 0.4*\text{REF A}$ 2-4
$S_4 = 0.6*\text{REF B} + 0.4*\text{REF E}$ 2-5
$S_5 = 0.7*\text{REF C} + 0.3*\text{REF D}$ 2-6
$S_6 = 0.4*\text{REF B} + 0.6*\text{REF E}$ 2-7
$S_7 = 0.5*S_1 + 0.4*S_5 + 0.1*\text{REF D}$ 2-8

In Equations 2-2–2-8, the mixing fraction of each initial water sample is given with a coefficient. Mass transfer to and from reacting phases is determined simultaneously with the mixing fractions, although each mass transfer is not considered in the example given in Figure 2-2.

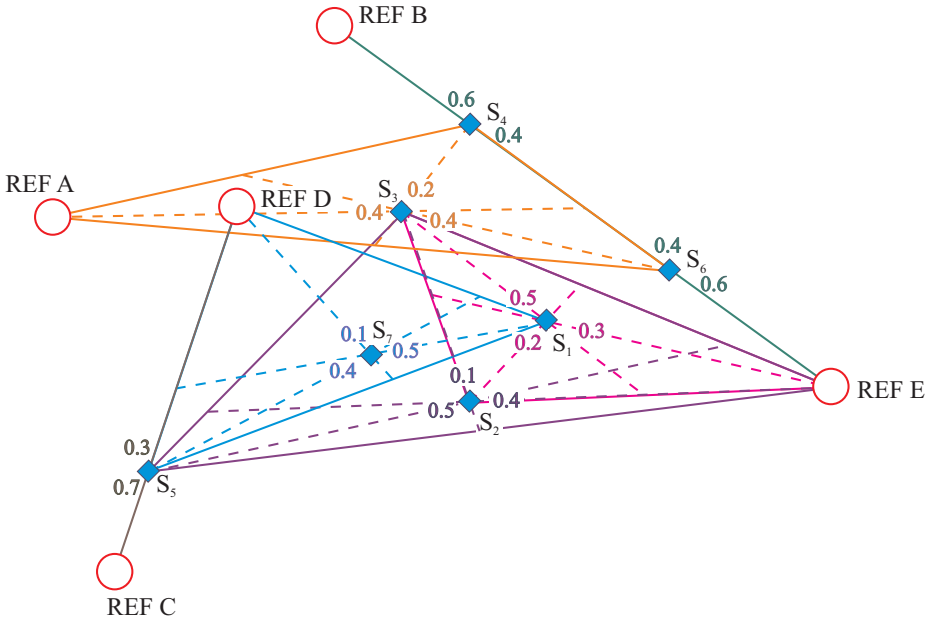

Figure 2-2. *Diagrammatic representation of the stepwise calculation of reference water type mixing fractions in the collected water samples. Samples used as initial types of water for a certain final water sample are related by solid tie-lines. The broken lines illustrate the approximate Euclidean distance of initial waters from a final water sample. Solid and broken lines, and mixing fractions, related to the same final water sample are represented by the same colour.*

The calculation of the mixing fractions of reference water types for each sample from Equations 2-2–2-8 is now straightforward. For example, in the case of the sample S_1, Equations 2-3 and 2-4 are first substituted into Equation 2-2, and then Equations 2-5, 2-6 and 2-7 are substituted into Equation 2-2. The results for all samples are thus:

$S_1 = 0.20*\text{REF A} + 0.15*\text{REF B} + 0.07*\text{REF C} + 0.03*\text{REF D} + 0.55*\text{REF E}$ 2-9
$S_2 = 0.04*\text{REF A} + 0.03*\text{REF B} + 0.35*\text{REF C} + 0.15*\text{REF D} + 0.43*\text{REF E}$ 2-10
$S_3 = 0.40*\text{REF A} + 0.28*\text{REF B} + 0.32*\text{REF E}$ 2-11
$S_4 = 0.60*\text{REF B} + 0.40*\text{REF E}$ 2-12
$S_5 = 0.70*\text{REF C} + 0.30*\text{REF D}$ 2-13
$S_6 = 0.40*\text{REF B} + 0.60*\text{REF E}$ 2-14
$S_7 = 0.10*\text{REF A} + 0.07*\text{REF B} + 0.32*\text{REF C} + 0.24*\text{REF D} + 0.27*\text{REF E}$ 2-15

As was noted in Section 2.2.2, analytical uncertainties are included in the calculations. These uncertainties are also reflected by the mixing fractions (see Appendices 1 & 2). In addition to representative mixing fraction results, the calculations give the minimum and maximum fractions possible within the defined analytical uncertainties. The minimum and maximum fractions of initial water samples can be entered into the calculation chain, just as the representative values. The minimum and maximum fractions of the reference water types for each sample give the cumulative extreme fractions possible within the analytical uncertainties assigned to each sample along the calculation chain. Therefore, as the chain of intermediate samples towards the reference water types becomes longer, the range of the lower and upper limits of mixing fractions inevitably becomes wider for a particular sample. In the above example (Fig. 2-2) mixing fraction uncertainties related to sample 1 (S_1) would probably be higher than, for example, the uncertainties related to sample 5 (S_5).

The example illustrated in Figure 2-2 gives an approximate view of the mixing calculations. In practice, the greater the number of steps close to the reference water types, the more realistic the results, i.e. pure mixing between two reference waters is avoided better. The reference water types presented in Table 2-1 are shown in Figure 2-3 together with groundwater samples taken prior to the Äspö HRL excavations (blue diamonds), and the samples taken during and after major excavation activities (grey squares). The arrows illustrating the groundwater evolution trends during the history of Äspö are in accordance with Figure 2-1. The oldest reference water types locate at the stating points of the evolution trends, and more recent reference water types are mixed into systems as samples get younger. In Figure 2-3, baseline samples used to determine the hypothetical flow paths to the prototype repository near-field samples are labelled with their ID acronyms.

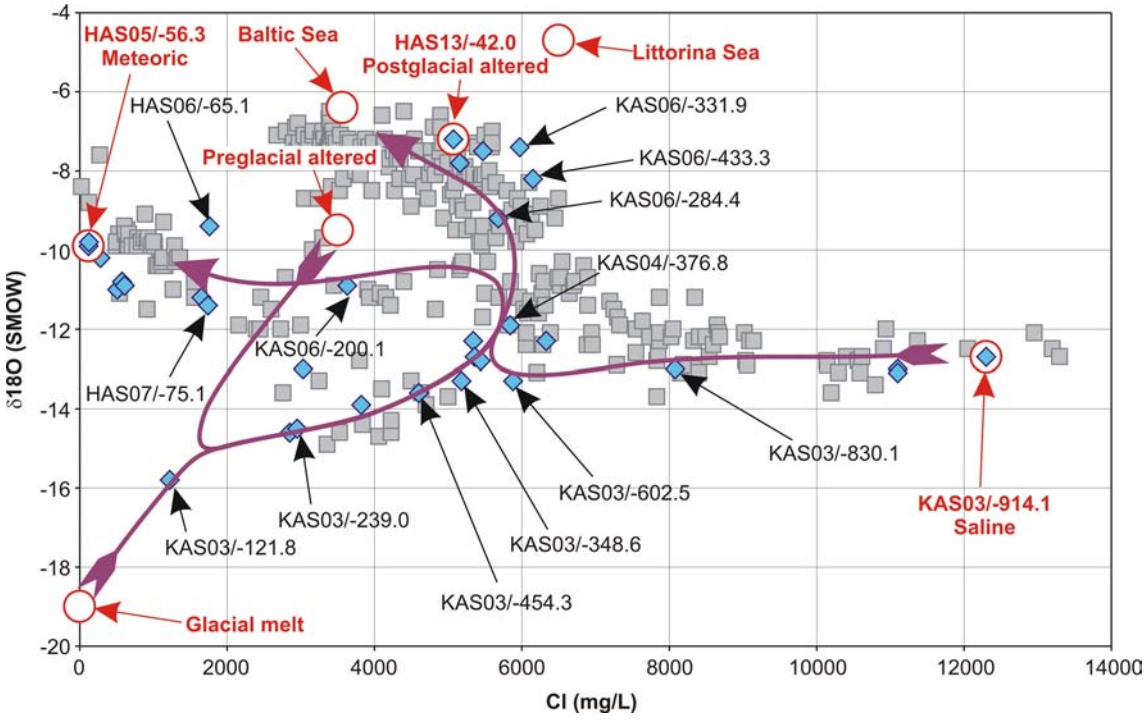

Figure 2-3. *A schematic overview of the mixing evolution at Äspö. The assumed evolution trends below sea and land areas are represented by purple arrows. Äspö baseline samples prior to the HRL excavations are represented by blue diamonds, and a set of disturbed Äspö samples is shown by grey squares.*

3 Results

The geochemical groundwater data were divided into two sets. Samples taken prior to excavation activities on the island of Äspö are considered baseline samples. This set of data is used as a geochemical frame that must be solved before other samples can be interpreted. In the current case, the other set of data consists of the samples collected in the prototype repository near field during the years 1998–2004. A part of the near field samples have been collected during the time when the experiment was being set up and the canister heaters were gradually turned on. Soon after the sampling campaigns considered here one heater failed (Dec. 2004) and another began to work deficiently (Goudarzi & Johannesson 2005, 2006).

3.1 Baseline conditions

The baseline samples were collected between August 8, 1987 and July 3, 1989. The reference water mixing fractions and mass transfer of reacting phases were calculated for 13 baseline samples. Additionally, three samples (HAS05/-56.3m, HAS13/-42.0m and KAS03/-914.1m, see Section 2.2.3) from the baseline data were chosen as reference water types.

Based on the judgement rules outlined in Table 2-1 and the calculation method illustrated in Section 2.3, the chosen baseline samples were related to each other. The flow paths for baseline samples are presented in Figure 3-1. The flow paths considered here are hypothetical in the sense that no physical path was required between the interrelated sampling points. The aim is to describe the general evolution of water in the bedrock. It is assumed that if stepwise data were available along all the physical flow paths related to the chosen undisturbed samples, we would find chemical evolution of groundwater analogous to that described here with hypothetical flow paths.

The mixing fractions of the reference water types in the 13 baseline samples studied are presented in Table 3-1. The variation for each calculated representative mixing fraction is also given. The variance limits give a qualitative level of confidence for the estimates of the representative mixing fractions. Characteristically, as a step-wise flow path such as that illustrated in Figure 3-1, becomes longer, the confidence range becomes wider. The same mixing fractions, but with cumulative mass transfer for each baseline sample, are presented in Table 3-2. The approximate cumulative mass transfer was calculated by adding the step-wise transfer originating from the complete flow path of each sample (see Fig. 3-1). The original quantitative mass-transfer results generated during each individual flow path step are presented in Appendix 1.

The interpretation of Table 3-2 is easier if a correlation matrix is calculated. The number of baseline samples studied is small. It can be also suspected that the variables presented do not obey linear relations or normal distributions. Therefore, Spearman rank correlation was chosen as the correlation method (Table 3-3). The significance of correlations was studied with the hypothesis of no correlation against the alternative that there is a non-zero correlation. If a no-correlation p-value related to an individual rank correlation value is small enough, then the studied correlation is significantly different from zero. Only correlations giving p-value less than 0.05 are presented in Table 3-3.

Using rank correlation means that the coefficients shown in Table 3-3 cannot be read in terms of linear interdependence, but coefficient value designate only the “significance” of a positive/negative correlation.

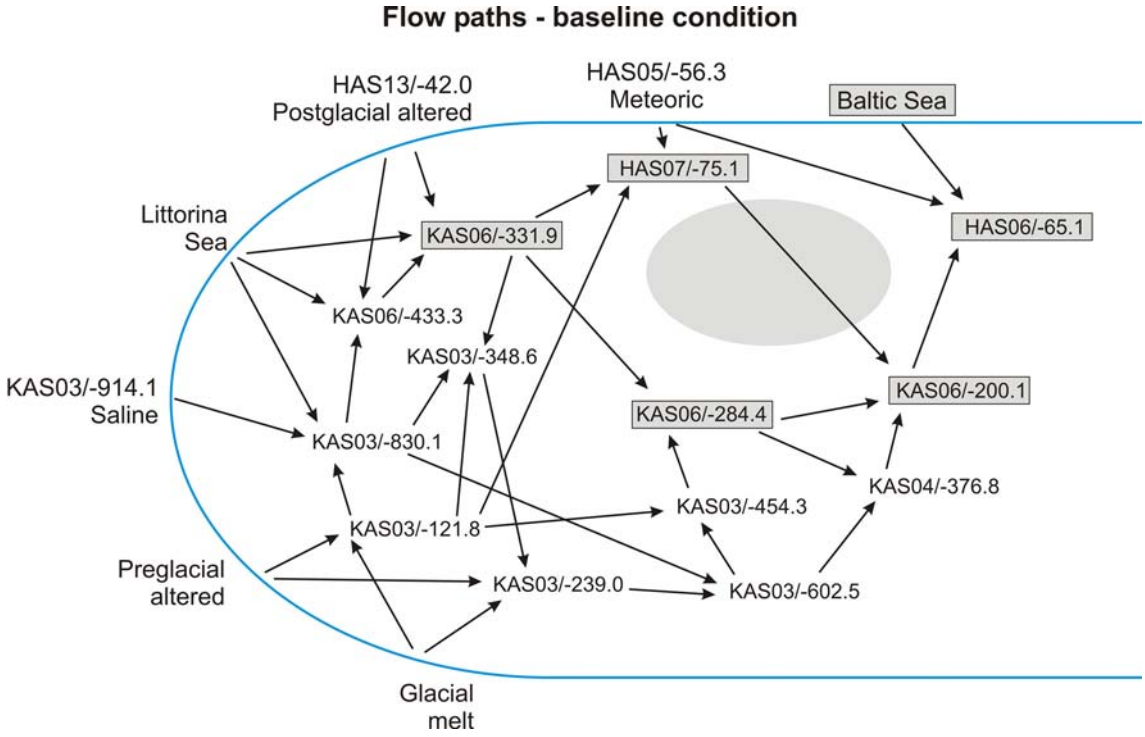

Figure 3-1. *Hypothetical flow paths used in mass-transfer modelling. The blue line separates reference water types from the rest of the data. Flow paths are indicated by black arrows. The compositions of the near-field samples (shaded area) were reproduced with the aid of baseline samples (IDs in shaded boxes).*

Table 3-1. Reference water type mixing fractions (in percent) in the studied baseline Äspö water samples. Estimated minimum and maximum fractions are given after each representative value. The representative fractions in boldface on one line add up to 100.

Sample	Meteoric			Baltic Sea			Postglacial alt.			Littorina Sea			Glacial melt			Preglacial alt.			Saline		
		min	max		min	max		min	max		min	max		min	max		min	max		min	max
HAS05/-56.3	**100.0**																				
HAS13/-42.0							**100.0**														
KAS03/-914.1																			**100.0**		
HAS06/-65.1	**53.3**	50.9	56.7	**30.4**	29.9	31.2	**5.3**	2.1	10.1	**1.3**	0.3	3.3	**4.7**	1.8	8.3	**2.4**	0.9	4.9	**2.6**	0.6	6.1
HAS07/-75.1	**47.0**	40.5	57.1				**13.7**	11.1	17.9	**2.6**	1.6	4.2	**23.3**	15.8	26.5	**11.5**	8.1	13.9	**1.9**	1.3	3.0
KAS06/-200.1	**24.8**	18.3	33.3				**24.6**	10.4	44.1	**6.0**	1.6	14.6	**21.5**	9.1	36.4	**11.2**	4.7	21.4	**11.8**	2.8	26.7
KAS06/-284.4							**57.6**	49.9	61.0	**11.8**	7.4	16.0	**11.5**	9.0	16.0	**6.0**	4.7	9.3	**13.1**	9.9	18.3
KAS03/-454.3							**1.2**	0.3	2.2	**4.4**	2.3	7.9	**44.2**	35.2	51.3	**23.6**	18.4	30.9	**26.7**	21.4	33.5
KAS04/-376.8							**16.6**	12.6	20.9	**7.9**	4.3	13.0	**27.4**	21.5	33.1	**15.5**	11.5	21.8	**32.6**	25.6	40.0
KAS03/-121.8													**66.9**	65.0	66.9	**33.1**	33.1	35.0			
KAS03/-239.0							**4.5**	1.1	7.3	**2.6**	0.8	5.4	**50.2**	40.5	56.5	**31.3**	22.6	43.0	**11.5**	6.5	17.9
KAS03/-348.6							**11.4**	3.5	16.2	**6.5**	2.6	12.0	**35.5**	28.8	43.6	**17.6**	14.7	22.8	**29.1**	20.6	39.5
KAS06/-433.3							**51.4**	42.6	57.3	**22.6**	15.4	29.0	**6.3**	5.1	7.8	**3.1**	2.6	4.1	**16.6**	12.9	21.2
KAS06/-331.9							**70.8**	65.5	74.6	**13.6**	9.2	17.4	**3.8**	3.0	4.7	**1.9**	1.5	2.5	**10.0**	7.7	12.7
KAS03/-602.5							**1.8**	0.4	3.0	**6.5**	3.5	10.8	**33.2**	27.7	37.4	**19.0**	14.9	25.1	**39.6**	33.3	45.7
KAS03/-830.1										**9.1**	5.5	13.9	**22.1**	20.7	22.9	**11.0**	10.5	12.0	**57.9**	52.4	62.2

Table 3-2. Calculated representative reference water mixing fractions (in percent, cf. Table 3-1) and cumulative mass transfer (in mmol/L) for the baseline samples from Äspö. The results of original mass-transfer calculations are presented in Appendix 1.

Sample	Meteoric	Baltic Sea	Post-glacial alt.	Littorina Sea	Glacial melt	Pre-glacial alt.	Saline	Calcite	Dolomite	"CH_2O"	NaX	KX	CaX_2	MgX_2	Goethite	FeX_2	Pyrite
HAS06/-65.1	53.3	30.4	5.3	1.3	4.7	2.4	2.6	-1.97	0.05	0.53	-0.23	-0.42	3.02	-1.69	1.14	-1.01	-0.07
HAS07/-75.1	47.0		13.7	2.6	23.3	11.5	1.9	-2.90	0.34	0.32	-2.69	-0.13	3.36	-0.67	1.29	-1.28	
KAS06/-200.1	24.8		24.6	6.0	21.5	11.2	11.8	-3.91	0.23	2.40	-1.04	-0.30	3.47	-0.88	2.43	-1.93	-0.51
KAS06/-284.4			57.6	11.8	11.5	6.0	13.1	-2.48	0.03	1.59	0.23	-0.69	4.49	-2.86	1.71	-1.41	-0.33
KAS03/-454.3			1.2	4.4	44.2	23.6	26.7	-2.45	0.17	1.68	1.22	-0.05	1.64	-1.05	1.54	-1.17	-0.37
KAS04/-376.8			16.6	7.9	27.4	15.5	32.6	-2.61	0.19	1.58	1.39	-0.29	2.74	-2.02	1.60	-1.27	-0.34
KAS03/-121.8					66.9	33.1		-0.11		0.02		0.06	0.70	-0.65	0.08	-0.09	
KAS03/-239.0			4.5	2.6	50.2	31.3	11.5	-5.40	0.63	3.83	4.68	0.02	0.67	-0.76	3.12	-2.26	-0.87
KAS03/-348.6			11.4	6.5	35.5	17.6	29.1	-2.30		1.57	3.26	-0.22	1.67	-1.89	1.62	-1.29	-0.33
KAS06/-433.3			51.4	22.6	6.3	3.1	16.6	-0.88		0.13		-0.96	4.99	-3.97	0.53	-0.54	
KAS06/-331.9			70.8	13.6	3.8	1.9	10.0	-0.89		0.14		-0.79	3.33	-2.38	0.54	-0.56	
KAS03/-602.5			1.8	6.5	33.2	19.0	39.6	-2.66	0.25	1.58	1.82	-0.15	2.10	-1.72	1.55	-1.21	-0.34
KAS03/-830.1			0.0	9.1	22.1	11.0	57.9	-0.39		0.06		-0.25	1.88	-1.51	0.23	-0.23	

Table 3-3. Pair-wise Spearman correlations for the data given in Table 3-2. Only significant correlations are presented, p<0.05.

RHO	Meteoric	Baltic Sea	Post-glacial alt.	Littorina Sea	Glacial melt	Pre-glacial alt.	Saline	Calcite	Dolomite	"CH_2O"	NaX	KX	CaX_2	MgX_2	Goethite	FeX_2	Pyrite
Meteoric	1																
Baltic Sea	0.626	1															
Postglacial alt.			1														
Littorina Sea			0.588	1													
Glacial melt			-0.691		1												
Preglacial alt.			-0.660	-0.568	0.989	1											
Saline							1										
Calcite								1									
Dolomite								-0.916	1								
"CH_2O"								-0.834	0.696	1							
NaX	-0.727										1						
KX			-0.776	-0.730	0.923	0.918						1					
CaX_2			0.795		-0.819	-0.775					-0.566	-0.819	1				
MgX_2			-0.641	-0.854	0.599	0.615						0.813		1			
Goethite								-0.852	0.622	0.922					1		
FeX_2								0.890	-0.667	-0.850						1	
Pyrite								0.745	-0.650	-0.948					-0.850	0.731	1

The upper left section of Table 3-3 shows correlations between the reference water types. Meteoric reference water correlates positively with fresh Baltic Sea water. This is logical, since both meteoric and Baltic Sea references are used to make up two baseline samples (Fig. 3-1). In principle, the sources of meteoric and Baltic Sea water are independent. However, as they both infiltrate from the surface, they are easily mixed together. The surficial nature of these reference waters is emphasized by the fact that they do not correlate with other types of reference water.

The close relation between the Littorina Sea and the postglacial altered reference water is expected (Table 3-3). The relation between the two was pointed out in Section 2.2.3. In principle, the sum of the Littorina Sea and postglacial altered water fractions in Table 3-2 should represent the complete seawater contamination of baseline samples from the Äspö deglaciation stage until the beginning of the present Baltic Sea stage. Both Littorina Sea and postglacial altered waters exhibit negative correlation to preglacial altered reference water. According to Table 3-3, only postglacial altered water exhibits a negative correlation to glacial melt water. Postglacial altered water appears to have greater variability than Littorina Sea water, and is therefore better correlated (cf. Table 3-2).

Glacial meltwater correlates strongly and positively to preglacial altered water (Table 3-3). This is as expected because baseline samples with high glacial affinity were used to estimate the preglacial altered water composition (cf. Sec. 2.2.3). Figures 2-3 and 3-1 also give some idea of the close relation between these two waters.

The deep independent source of saline reference water is emphasized by the fact that this reference water is not significantly correlated to any other water type (Table 3-3). In this respect, saline reference water resembles the surficial reference water types (meteoric and Baltic Sea).

The lower left section of Table 3-3 indicates that significant utilisation of postglacial altered or Littorina Sea water references to obtain a final water composition leads to significant K^+ and Mg^{2+} absorption into solid phases. The use of postglacial altered water as a mixing source also indicates the release of Ca^{2+} from solid phases. These results are expected for reference waters with high seawater affinity. Similarly, it is reasonable that significant utilisation of present Baltic Sea as a mixing source leads to Na^+ adsorption (coupled with K^+ and Mg^{2+} adsorption, and Ca^{2+} release). This mass transfer actually occurs in sample HAS06/65.1 (Table 3-2). However, only one baseline sample (HAS06/65.1) consists of Baltic Sea and meteoric sources, and therefore the correlation in Table 3-3 remains insignificant. In the case of older seawater, both postglacial altered and Littorina Sea waters are always used together as mixing sources in the same samples. Apparently, this “screens” the expected mass transfer of Na^+ since the postglacial reference water is already altered in this respect (cf. Table 2-1).

The results presented in Table 3-3 imply that significant use of glacial meltwater and preglacial altered water as mixing sources leads to counterbalancing mass transfer compared with seawater mixing cases. In other words, Ca^{2+} is adsorbed while K^+ and Mg^{2+} are released into the final water. Considering the wider view of the past Äspö water–rock interaction, the recharge of exchange sites with Ca^{2+} during glacial times is reasonable, since these reserves are used later for Na^+ adsorption during the seawater stages (see Fig. 2-1).

Extensive use of meteoric reference water as a mixing source leads to significant adsorption of Na^+. This is reasonable, as the Na^+ concentration in the meteoric reference water is relatively high (Table 2-1). The counter-balancing mass transfer does not satisfy the criterion required for statistical significance. However, the directions of mass transfer can be seen from Table 3-2 (see especially samples HAS07/-75.1 and KAS06/-200.1).

Finally, the lower left corner of Table 3-3 indicates that there is no significant correlation between saline reference water and geochemical processes. This is in accordance with the past evolution at Äspö (Fig. 2-1). Deep saline water should be well equilibrated with its surroundings. Furthermore, other reference waters cannot reach the saline water without going through the necessary transport and coupled geochemical processes on the way to greater depths.

The lower right section of Table 3-3 illustrates the correlations between the geochemical processes. The correlations are to some degree self-explanatory since they are implemented within the inverse modelling tool. In the case of cation exchange, it is expected that, being major cations, Na^+ and Ca^{2+} correlate mostly negatively with each other. However, correlations between the cation-exchange sites are not straightforward, as can be seen from Table 3-2. This is because the mass transfers presented in Table 3-2 are cumulative but approximate, i.e. in most cases, several partially contradictory steady-state steps (cf. Fig. 3-1) have been added to give each value. The quantitative, step-wise mass-transfer results are presented in Appendix 1.

The relations between the carbonate minerals and organic matter show that calcite precipitation and consumption of organic matter are strongly related. Dolomite (like organic matter) is only allowed to dissolve in the modelling calculations. Therefore, dolomite is bound to be a source of Mg^{2+} in the calculations. However, consumption of organic matter is an important process used to adjust bicarbonate levels between initial waters and the final water.

The correlations between goethite, FeX_2 (iron in ion-exchange sites) and pyrite also originate mainly from the modelling constrains. Goethite and pyrite are allowed only to dissolve and precipitate, respectively. These processes produce Fe^{2+} and consume the S^{2-} formed from solutions. Reactions are needed to adjust the dissolved sulphate level between that in the initial waters and that in the final water produced. FeX_2 acts as an additional sink for Fe^{2+}.

The positive relations between calcite and pyrite, and between goethite and organic matter, indicate that the separate processes usually proceed in the same direction. In other words, calcite precipitates as organic matter is consumed, and pyrite precipitates as goethite dissolves.

3.2 Prototype repository near-field samples

The prototype repository is surrounded by several groundwater, geochemical monitoring points. Of these sampling locations KA3539G, KA3542G01, KA3548A01, KA3554G01, KA3554G02, KA3566G02, KA3590G01, KG0021A01 and KG0048A01 were studied in detail. Groundwater samples from these locations form time series from

August, 1998 to November, 2004. Each location produced two to four geochemically analysed monitoring samples. The $\delta^{18}O$ values and Cl concentrations for the sampling locations are presented in Figure 3-2.

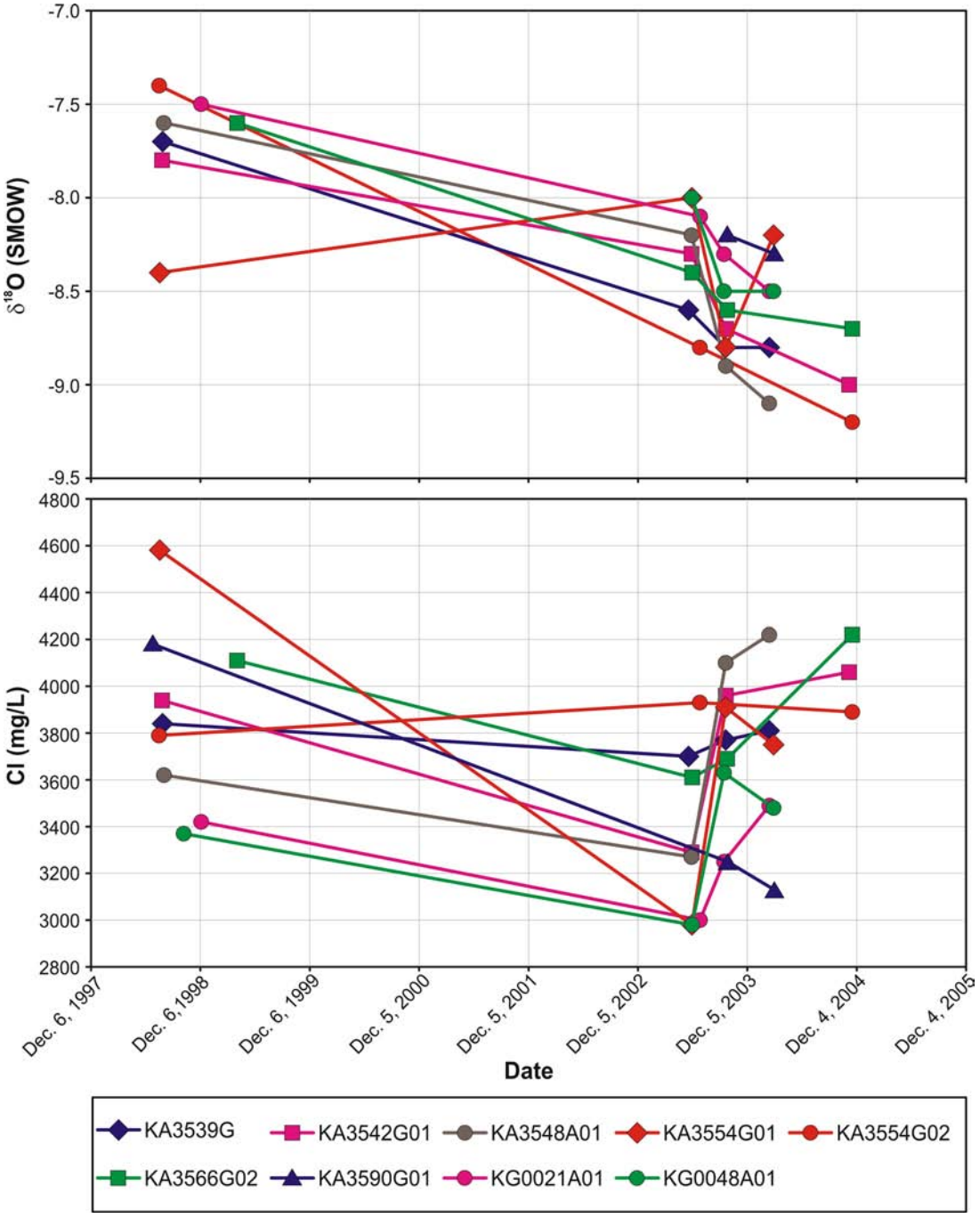

Figure 3-2. *Time-series of samples from the Äspö HRL fracture locations in the close vicinity of the excavated prototype repository facility.*

During the time span considered, temperature and pressure gradients were induced within the prototype repository. In the Section 1 of the repository, the first heater (canister 1) was activated on Sep. 17, 2001. In the Section 2, the first heater (canister 5) was activated on May 8, 2003. In the last deposition hole (canister 6) heating began on May 23, 2003 (Goudarzi & Johannesson 2005, 2006). The outer concrete plug closing the prototype repository tunnel was finalised on Sept. 11, 2003. However, this plug was not sealed until October 2004. The drainage was closed from both prototype repository compartments on Nov. 1, 2004, and the pressure build-up began in the tunnel backfill.

Oxygen isotope ratios of water are known to be susceptible to temperature changes. If water undergoes evaporation, the residual water becomes progressively enriched in the heavier isotope, ^{18}O. In the data presented in Figure 3-2, the possible ^{18}O enrichment as a consequence of temperature rise remains ambiguous because during the activation of heaters in Section 1 no ^{18}O isotope measurements were done in the prototype repository near-field (cf. Fig. 3-2). The data available from the latter half of 2003 indicate only changes in the hydrological flow conditions (tunnel backfilling, construction of plugs), since the enrichment of the ^{18}O isotope is coupled to the increase in chlorine concentration.

In the inverse modelling calculations described above it was assumed that heating in the prototype repository did not cause isotopic fractionation in the near-field bedrock groundwater. The changes in isotopic ratios and chlorine content are assumed to originate exclusively from groundwater arising from changes in hydraulic gradients in the surroundings of the prototype repository.

Figure 3-3 illustrates the studied near-field samples in the Cl-^{18}O plot. Purely graphical interpretation gives the impression that the samples collected from a depth of around 450 metres, plot to areas in the graph where shallow or moderate depth baseline samples dominate. The most dilute near-field samples seem to have strong Baltic Sea affinity, and affinity to surficial meteoric waters can also be suspected. The most saline samples indicate mixing with older Äspö waters (Fig. 2-3). By taking into account the sampling depths of the referred baseline samples (Fig. 3-3, the latter part of the labelled acronyms indicate the sampling depth), it appears that the major source of water for the near-field sampling locations studied is above the repository.

Inverse modelling calculations for the near-field samples were carried out with the aid of six baseline samples presented in Figs. 3-1 and 3-3. Table 3-4 summarises the representative calculated mixing fractions together with the estimated maximum and minimum fractions for the near-field samples. The results presented in Table 3-4 give the impression that the changes in fractions in all samples, and within individual time series are moderate. The largest contribution to each studied sample is from the Baltic Sea. On average, 51% mixing of Baltic Sea water is needed. The second largest contributors to the samples are the relic seawater sources within the Äspö bedrock. Postglacial altered and Littorina Sea waters contribute together, on average, 19.8% to the observed prototype near-field waters. The surficial meteoric source contributes an average of 12.7% to the final observed water compositions. Other reference water sources are small contributors. Glacial melt, preglacial altered and saline water sources account for, on average, 7.9%, 4.1% and 4.4%, respectively, of the final water compositions.

The range in representative fractions can be fairly large, as seen in Table 3-4. The reason for the fluctuations in the upper and lower limits is the same as in the baseline sample calculations. The more steps a flow path contains, the broader the variation limits tend to be. In respect of mass transfers, an initial sample having more calculation steps behind can be more favourable for a final water calculation but a trade-off can be that the calculation result is more uncertain. For example, it may be favourable to change the initial sample HAS07/-75.1 to KAS06/-200.1 (see Fig. 3-3) in an inverse calculation where other initial waters apart from meteoric water remain the same. However, the variance becomes broader as more steps have been used to calculate the composition of KAS06/-200.1 than HAS07/-75.1 (cf. Fig. 3-1).

Table 3-5 summarises the representative mixing fractions and approximate cumulative mass transfer. Table 3-5 is analogous to Table 3-2, i.e. all contributions to mass transfer in the complete flow path used to reach the final sample were added. The presentation of sums may lead to ambiguities in certain cases, e.g. calcite may first dissolve and then precipitate in subsequent steady-state steps, or cation-exchange processes may exhibit counterbalancing mass transfer in successive steps. However, in the current study the general overview of the mass transfer is logical. Moreover, Table 3-5 gives an estimate of the amount of minerals dissolved and precipitated as water is transported from the sources to the surroundings of the prototype repository. These estimates may have implications on possible fracture sealing/erosion effects if the hydraulic conditions remain as they are now, for a long time at the Äspö HRL (cf. e.g. Luukkonen 2006).

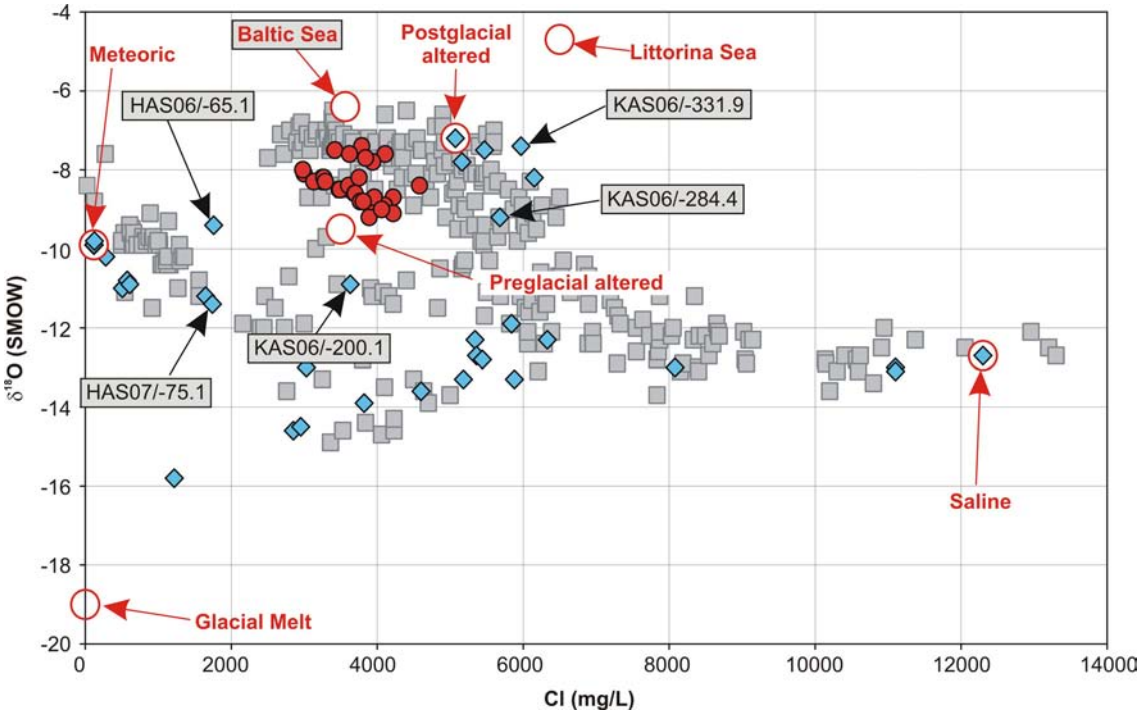

Figure 3-3. *Prototype repository near-field samples (red dots) in the Cl vs. ^{18}O plot. Äspö baseline samples prior to the HRL excavations are represented by blue diamonds and a set of disturbed Äspö samples are shown by grey squares. For further details see Figure 2-3. Labelled baseline samples were used for inverse mass-transfer calculations of the near-field samples.*

Table 3-4. Reference water type mixing fractions (in percent) in the studied prototype repository near-field samples. Estimated minimum and maximum fractions are given after each representative value. Values of representative fractions in boldface add up to 100 on each line.

Sample	Date	Meteoric			Baltic Sea			Postglacial alt.			Littorina Sea			Glacial melt			Preglacial alt.			Saline		
			min	max		min	max		min	max		min	max		min	max		min	max		min	max
KA3539G	Aug. 2, 1998	**10.4**	7.1	17.1	**51.8**	39.5	59.7	**21.4**	16.8	28.8	**4.1**	2.4	6.7	**6.2**	3.4	9.4	**3.1**	1.8	4.9	**3.0**	2.0	4.9
	May 23, 2003	**13.1**	8.0	18.9	**46.4**	38.5	53.4	**18.7**	12.4	25.2	**3.8**	1.8	6.4	**9.4**	5.0	13.9	**4.8**	2.5	7.6	**3.9**	2.3	6.8
	Sept. 24, 2003	**9.7**	5.8	18.0	**49.0**	41.2	53.2	**16.5**	3.3	36.8	**3.8**	0.5	11.3	**9.8**	2.9	23.1	**5.1**	1.5	13.5	**6.2**	0.9	18.3
	Feb. 16, 2004	**10.5**	6.1	16.9	**49.5**	44.7	54.1	**15.2**	3.5	33.6	**3.5**	0.5	10.3	**10.0**	3.0	21.4	**5.2**	1.6	12.6	**6.1**	1.0	16.9
KA3542G01	July 31, 1998	**19.6**	11.9	27.0	**45.4**	23.5	65.5	**22.5**	15.4	31.6	**4.4**	2.2	7.8	**2.8**	1.1	5.7	**1.4**	0.6	3.2	**3.8**	1.9	7.5
	June 2, 2003	**14.7**	8.8	22.6	**53.6**	43.2	63.8	**12.9**	7.5	19.5	**2.6**	1.1	4.9	**9.0**	4.3	13.8	**4.5**	2.2	7.4	**2.6**	1.3	4.9
	Sept. 24, 2003	**8.3**	4.4	16.3	**47.5**	38.5	52.5	**19.2**	5.7	39.8	**4.3**	0.9	11.9	**9.3**	2.8	22.6	**4.9**	1.4	13.2	**6.5**	1.3	18.5
	Nov. 9, 2004	**9.9**	5.5	16.3	**40.2**	34.8	45.7	**21.2**	8.6	40.6	**4.7**	1.3	12.1	**10.9**	3.7	22.8	**5.7**	1.9	13.4	**7.3**	1.9	18.8
KA3548A01	Aug. 6, 1998	**17.8**	13.3	25.1	**54.5**	35.0	68.8	**17.6**	13.0	25.8	**3.5**	1.8	6.4	**2.4**	1.1	5.0	**1.2**	0.5	2.9	**3.1**	1.6	6.3
	June 2, 2003	**8.7**	4.8	14.4	**49.9**	37.5	62.0	**19.4**	9.5	34.7	**4.2**	1.4	9.9	**8.1**	2.7	16.8	**4.2**	1.4	9.8	**5.6**	1.5	14.2
	Sept. 24, 2003	**8.1**	4.8	14.5	**43.9**	38.1	47.2	**21.6**	9.2	39.5	**4.7**	1.4	11.7	**9.7**	3.6	21.2	**5.0**	1.8	12.4	**6.9**	2.0	17.7
	Feb. 16, 2004	**7.6**	4.4	11.2	**35.7**	31.1	37.7	**26.9**	16.8	41.9	**5.8**	2.5	12.0	**10.4**	4.7	19.4	**5.4**	2.5	11.4	**8.0**	3.5	17.1
KA3554G01	June 3, 2003	**15.4**	11.3	23.9	**61.4**	49.7	71.1	**8.6**	3.7	15.1	**1.6**	0.5	3.5	**7.8**	4.4	11.6	**3.9**	2.3	6.1	**1.2**	0.4	2.6
	Sept. 24, 2003	**8.9**	4.9	15.7	**45.9**	40.2	50.7	**19.3**	6.4	38.5	**4.3**	1.0	11.5	**9.8**	3.1	21.8	**5.1**	1.6	12.8	**6.6**	1.5	17.9
	March 2, 2004	**15.9**	7.9	22.7	**46.3**	28.2	63.2	**20.6**	13.6	28.4	**4.3**	2.0	7.7	**5.2**	2.7	9.7	**2.7**	1.4	5.7	**5.1**	2.7	9.7
KA3554G02	July 21, 1998	**16.4**	9.2	23.7	**57.7**	40.3	80.2	**16.4**	10.0	24.2	**3.2**	1.4	6.1	**2.2**	0.8	4.7	**1.1**	0.4	2.7	**2.9**	1.2	6.0
	June 30, 2003	**10.6**	6.1	16.3	**49.3**	40.1	53.3	**15.2**	5.6	32.8	**3.5**	0.9	10.1	**10.1**	3.4	20.8	**5.3**	1.8	12.2	**6.1**	1.4	16.4
	Nov. 19, 2004	**9.5**	6.8	12.8	**37.0**	35.9	37.0	**23.6**	16.2	33.0	**5.2**	2.4	9.8	**11.1**	5.6	18.2	**5.8**	2.9	10.7	**7.8**	3.5	15.1
KA3566G02	April 8, 1999	**5.6**	2.0	11.1	**56.1**	45.3	65.8	**20.6**	8.4	39.3	**4.2**	1.2	10.6	**5.7**	1.3	13.7	**2.9**	0.7	8.0	**4.8**	1.2	13.1
	June 4, 2003	**10.8**	6.6	15.9	**56.4**	52.4	63.7	**10.7**	3.8	21.0	**2.6**	0.6	6.9	**9.4**	3.3	17.3	**4.9**	1.7	10.2	**5.2**	1.0	12.7
	Sept. 29, 2003	**12.3**	7.7	16.5	**50.5**	50.4	57.7	**12.2**	4.4	21.9	**3.0**	0.7	7.2	**10.6**	3.8	18.1	**5.5**	2.0	10.6	**5.9**	1.2	13.2
KA3590G01	Sept. 30, 2003	**13.9**	8.2	22.3	**55.8**	45.3	66.0	**12.5**	7.2	19.3	**2.5**	1.1	4.9	**8.5**	4.1	13.6	**4.3**	2.1	7.3	**2.5**	1.3	4.9
	March 4, 2004	**15.4**	10.1	23.9	**54.6**	46.2	64.7	**11.8**	6.8	18.3	**2.4**	1.0	4.6	**9.1**	4.7	13.9	**4.5**	2.4	7.5	**2.3**	1.1	4.5
KG0021A01	Dec. 9, 1998	**17.8**	12.7	25.1	**61.8**	43.1	78.4	**12.4**	7.4	19.9	**2.5**	1.1	5.1	**2.1**	0.8	4.7	**1.1**	0.4	2.7	**2.3**	1.0	5.3
	June 30, 2003	**21.1**	12.9	33.5	**60.7**	45.1	74.3	**5.9**	1.3	16.0	**1.5**	0.2	5.3	**5.2**	1.2	13.2	**2.7**	0.6	7.8	**2.9**	0.4	9.7
	Sept. 18, 2003	**14.3**	8.4	19.8	**55.2**	46.5	64.0	**12.4**	7.2	18.2	**2.5**	1.0	4.6	**8.7**	4.1	12.3	**4.4**	2.1	6.6	**2.5**	1.2	4.7
	Feb. 17, 2004	**14.3**	8.8	20.4	**50.2**	43.2	58.0	**15.3**	9.6	21.5	**3.1**	1.4	5.4	**9.3**	4.7	13.4	**4.7**	2.4	7.3	**3.1**	1.7	5.6
KG0048A01	June 3, 2003	**16.0**	10.4	22.8	**66.0**	60.1	74.2	**4.7**	2.9	7.1	**0.9**	0.4	1.7	**7.9**	4.1	10.6	**3.9**	2.1	5.5	**0.7**	0.3	1.2
	Sept. 18, 2003	**10.8**	7.9	16.5	**54.4**	43.3	56.6	**16.2**	11.0	22.6	**3.3**	1.6	5.8	**7.9**	4.7	12.2	**4.0**	2.4	6.7	**3.4**	2.0	6.1
	March 2, 2004	**13.8**	8.0	20.4	**47.6**	42.1	56.6	**17.3**	11.1	23.9	**3.5**	1.6	6.1	**9.5**	4.7	14.1	**4.8**	2.4	7.6	**3.6**	2.0	6.3

Table 3-5. Calculated representative reference water mixing fractions (in percent, cf. Table 3-4) and cumulative mass transfer (in mmol/L) for the prototype repository near-field samples from Äspö. The results of original mass-transfer calculations are presented in Appendix 2.

Sample	Date	Meteoric	Baltic Sea	Post-glacial alt.	Littorina Sea	Glacial melt	Pre-glacial alt.	Saline	Calcite	Dolomite	"CH_2O"	NaX	KX	CaX_2	MgX_2	Goethite	FeX_2	Pyrite
KA3539G	Aug. 2, 1998	10.4	51.8	21.4	4.1	6.2	3.1	3.0	-0.87	0.24	1.37	-0.59	-1.07	5.54	-4.64	0.42	-0.07	-0.36
	May 23, 2003	13.1	46.4	18.7	3.8	9.4	4.8	3.9	-1.46	0.21	1.39	-0.69	-0.95	5.59	-4.29	0.81	-0.48	-0.34
	Sept. 24, 2003	9.7	49.0	16.5	3.8	9.8	5.1	6.2	-1.82	0.09	2.24	-0.38	-0.95	5.78	-4.28	1.36	-0.83	-0.54
	Feb. 16, 2004	10.5	49.5	15.2	3.5	10.0	5.2	6.1	-1.84	0.22	1.86	-0.42	-0.97	5.63	-4.22	1.16	-0.72	-0.45
KA3542G01	July 31, 1998	19.6	45.4	22.5	4.4	2.8	1.4	3.8	-0.99	0.15	1.05	-0.08	-0.99	5.14	-4.28	0.58	-0.33	-0.26
	June 2, 2003	14.7	53.6	12.9	2.6	9.0	4.5	2.6	-1.27	0.30	1.51	-0.80	-0.98	5.21	-4.04	0.66	-0.28	-0.38
	Sept. 24, 2003	8.3	47.5	19.2	4.3	9.3	4.9	6.5	-1.76	0.18	1.77	-0.30	-0.94	5.33	-4.03	1.13	-0.69	-0.43
	Nov. 9, 2004	9.9	40.2	21.2	4.7	10.9	5.7	7.3	-2.06	0.14	1.63	-0.37	-0.87	5.92	-4.36	1.31	-0.94	-0.37
KA3548A01	Aug. 6, 1998	17.8	54.5	17.6	3.5	2.4	1.2	3.1	-0.85	0.02	1.63	-0.08	-1.09	5.03	-4.12	0.73	-0.33	-0.41
	June 2, 2003	8.7	49.9	19.4	4.2	8.1	4.2	5.6	-1.15	0.34	1.33	-0.94	-0.94	5.10	-3.96	0.53	-0.19	-0.34
	Sept. 24, 2003	8.1	43.9	21.6	4.7	9.7	5.0	6.9	-1.85	0.17	1.81	-0.28	-0.91	5.50	-4.14	1.19	-0.76	-0.43
	Feb. 16, 2004	7.6	35.7	26.9	5.8	10.4	5.4	8.0	-2.06	0.16	1.83	-0.24	-0.87	5.92	-4.44	1.34	-0.92	-0.43
KA3554G01	June 3, 2003	15.4	61.4	8.6	1.6	7.8	3.9	1.2	-1.34	0.08	3.03	-0.34	-1.08	4.96	-3.70	1.31	-0.55	-0.77
	Sept. 24, 2003	8.9	45.9	19.3	4.3	9.8	5.1	6.6	-1.86	0.21	1.99	-0.33	-0.90	5.47	-4.15	1.18	-0.71	-0.48
	March 2, 2004	15.9	46.3	20.6	4.3	5.2	2.7	5.1	-1.41	0.14	1.53	0.01	-0.96	5.41	-4.39	0.91	-0.55	-0.37
KA3554G02	July 21, 1998	16.4	57.7	16.4	3.2	2.2	1.1	2.9	-0.80	0.02	2.02	-0.07	-1.10	4.70	-3.88	0.74	-0.23	-0.52
	June 30, 2003	10.6	49.3	15.2	3.5	10.1	5.3	6.1	-1.88	0.20	1.76	-0.43	-0.96	5.60	-4.14	1.18	-0.77	-0.42
	Nov. 19, 2004	9.5	37.0	23.6	5.2	11.1	5.8	7.8	-3.64	0.10	3.11	-0.34	-0.84	6.43	-3.95	2.58	-1.89	-0.70
KA3566G02	April 8, 1999	5.6	56.1	20.6	4.2	5.7	2.9	4.8	-1.09	0.05	2.40	-0.24	-1.14	5.00	-4.00	0.93	-0.32	-0.62
	June 4, 2003	10.8	56.4	10.7	2.6	9.4	4.9	5.2	-1.72	0.10	2.33	-0.46	-1.01	5.38	-3.86	1.34	-0.78	-0.57
	Sept. 29, 2003	12.3	50.5	12.2	3.0	10.6	5.5	5.9	-1.92	0.25	2.00	-0.51	-0.90	5.05	-3.63	1.19	-0.71	-0.49
KA3590G01	Sept. 30, 2003	13.9	55.8	12.5	2.5	8.5	4.3	2.5	-1.24	0.34	1.75	-0.77	-0.98	5.22	-4.15	0.64	-0.19	-0.45
	March 4, 2004	15.4	54.6	11.8	2.4	9.1	4.5	2.3	-0.80	0.35	2.26	-0.33	-1.22	5.59	-4.97	0.46	0.15	-0.61
KG0021A01	Dec. 9, 1998	17.8	61.8	12.4	2.5	2.1	1.1	2.3	-1.02	0.02	2.12	-0.04	-1.14	5.07	-4.05	0.95	-0.43	-0.54
	June 30, 2003	21.1	60.7	5.9	1.5	5.2	2.7	2.9	-1.29	0.06	2.50	-0.25	-0.99	4.25	-3.13	1.13	-0.50	-0.63
	Sept. 18, 2003	14.3	55.2	12.4	2.5	8.7	4.4	2.5	-1.52	0.29	2.41	-0.28	-0.98	4.30	-3.31	0.97	-0.36	-0.62
	Feb. 17, 2004	14.3	50.2	15.3	3.1	9.3	4.7	3.1	-1.37	0.30	1.57	-0.79	-0.91	4.72	-3.53	0.72	-0.33	-0.40
KG0048A01	June 3, 2003	16.0	66.0	4.7	0.9	7.9	3.9	0.7	-0.98	0.40	1.85	-3.87	-1.02	5.88	-3.49	0.44	0.06	-0.50
	Sept. 18, 2003	10.8	54.4	16.2	3.3	7.9	4.0	3.4	-1.24	0.27	1.69	-0.56	-0.94	4.59	-3.58	0.69	-0.26	-0.43
	March 2, 2004	13.8	47.6	17.3	4.8	9.5	4.8	3.6	-1.41	0.29	1.66	-0.73	-0.89	5.01	-3.85	0.77	-0.35	-0.42

In Table 3-5, cation-exchange directions are as expected for final waters with significant contributions from seawater sources. Seawater contains abundant amounts of especially Na^+, K^+ and Mg^{2+}. It is expected that these elements will be subject to adsorption, while Ca^{2+} is a trade-off product that dissolves in water. Na^+ adsorption seems relatively small compared with Ca^{2+} dissolution. However, all mixing cases presented in Table 3-5 contain significant contributions from postglacial altered water in which the Na/Ca ratio has already been modified (cf. Table 2-1).

The relations between carbonates and organic matter obey the assumptions of organic matter respiration and low-temperature dissolution only character of dolomite (Tables 2-1, 3-5). Organic matter is consumed and calcite is precipitated. Dissolution of small amounts of dolomite mainly releases some Mg^{2+} into the water. Similarly, the mass transfer related to sulphate reduction and iron balance is also according to the assumptions, and moderate in extent. Goethite dissolves and produces dissolved iron. Contemporaneously, pyrite precipitates and consumes both sulphide and iron from the water. Iron cycle is mainly responsible for a small excess of dissolved iron that is adsorbed by exchange sites.

As a final illustration, some time series of water evolution in the surroundings of the prototype repository are presented in Figure 3-4. The four selected time-series contain 4 samples each, and the actual fractions can be found in Tables 3-4 and 3-5. All time series exhibit modest evolution with time at the locations sampled. There are long gaps from the end of 1998 until the beginning of 2003 when no sampling was performed. 2003 thus provides the first indication of changes at each sampled location. As was mentioned above, the construction of the prototype repository was finalised during 2003, and the plug closing the tunnel was finalised in September 2003. In view of the current results, it seems that the changes in the hydraulic conditions around the prototype repository are the main cause of changes in water fractions in the prototype repository near-field samples. However, in view of the number of samples from each sample location, the studied time-series are not long, although the time span considered is about seven years.

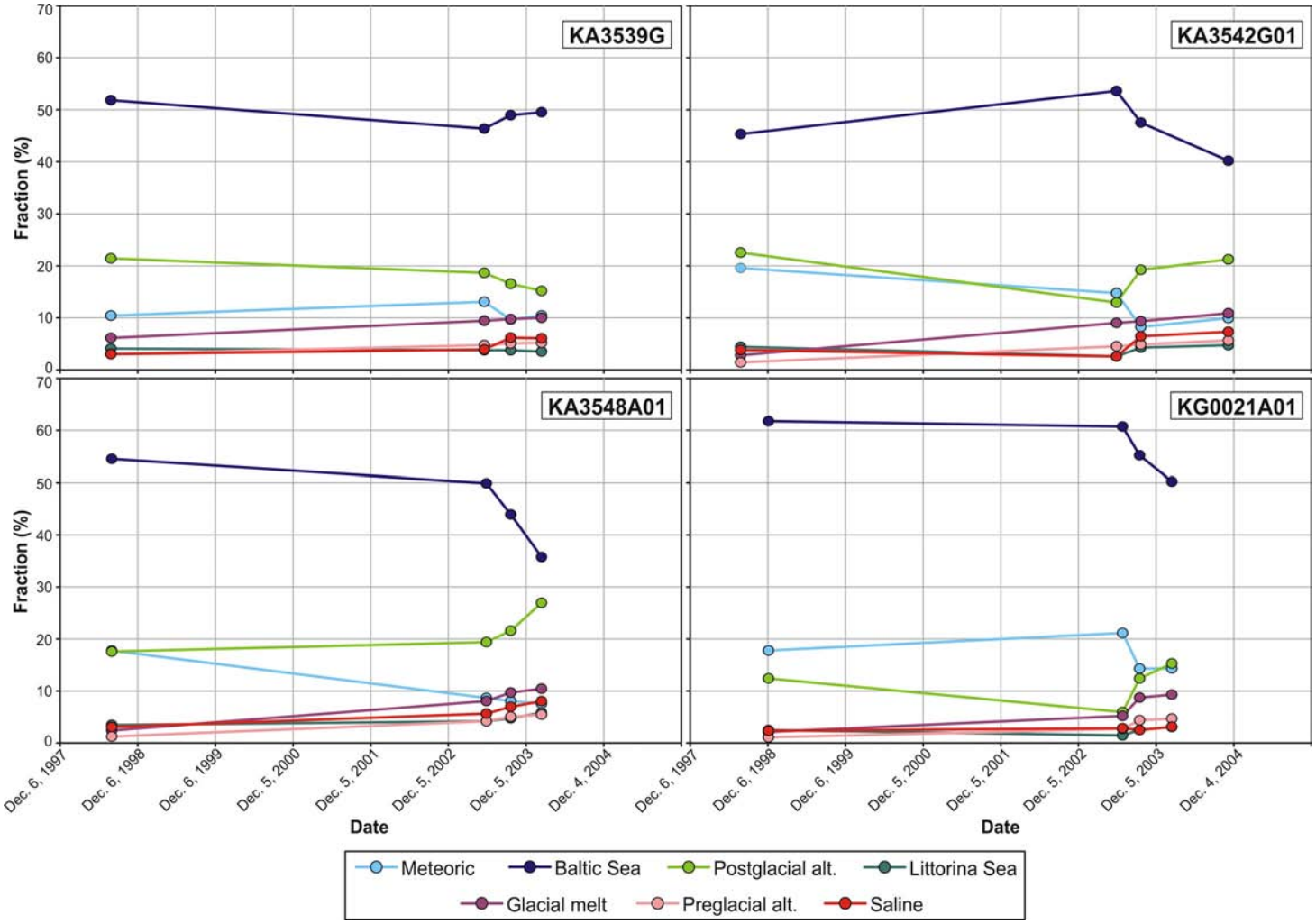

Figure 3-4. *Illustration of the evolution of reference water mixing fractions as a function of time in samples from the near field of the prototype repository (cf. Table 3-3).*

4 Conclusions

The aim of inverse modelling in the current study was to determine the mixing fractions of identified reference water types in the collected samples. The calculations also provided results on mass-transfer that indicate the extent of geochemical reactions needed for the reproduction of individual samples. The key results were presented in Tables 3-2 and 3-5 and the individual calculations can be found in Appendices 1 and 2.

The modelling problem is inverse regarding both individual samples and on the regional Äspö scale. In the case of an individual sample, the modelling makes quantitative deductions about the past (hence the term inverse approach). In other words, what kind of initial waters and geochemical phase reactions there have been to achieve existing final water. Regarding the whole Äspö Island, the past hydrogeological events are used for interpretations what kind of reference water types there have been available during the historical stages of water evolution. Chained inverse calculations require the interpretation of the succession of initial waters that have produced chained final groundwater compositions at Äspö.

The results for baseline samples seem reasonable considering the general history of Äspö. During glacial times Ca^{2+} is adsorbed onto exchange sites, while during seawater infiltration Na^{+} is adsorbed onto exchange sites. The release of Ca^{2+} is possible because of the previous recharging of Ca^{2+} onto exchange sites. There is also an additional logic in the historical succession of hydrogeological events. According to observations and the theory of cation exchange, dilution of solute (glacial times) causes the preferential adsorption of more highly charged cations (Ca^{2+}) onto the exchange sites (Appelo & Postma 1993, 2005). The inverse calculations done conform this preference, which in turn means release of Na^{+} from exchange sites into water. Conformably, the preglacial altered water is rich in Na^{+} (cf. Table 2-1) and is assumed to have equilibrated exchange sites before glacial melt. Therefore, the calculated mass transfer results calculated in this work, give more certainty to the preglacial altered water composition, which is basically only a rough assessment (cf. Pitkänen et al. 1999, Luukkonen & Kattilakoski 2001).

Another important result of baseline sample calculations is that no large mass transfers were related to the mixing of saline reference water. The greater the amount of saline water the smaller the cumulative mass transfers seem to be (cf. Table 3-3). The saline water is expected to be well equilibrated with the surrounding host rock. Saline water is located at depth. This means long flow paths and many equilibration possibilities for other water types before reaching the saline water. Saline water (Cl content 12,300 mg/L), used here as a saline reference, is also not the most saline water found in the Äspö-Laxemar area. The inevitable source of currently used saline reference water is even more saline brine. The genesis of this brine is considerably older than the history considered in this study (cf. Fig. 2-1). Also dilution occurred from brine to the used reference salinity is assumed to have occurred much earlier than the history considered here.

The compositions of the baseline samples were reproduced with the aid of seven types of reference water. However, three of these reference waters show almost complete seawater affinity. Littorina Sea water, postglacial altered water and present Baltic Sea water cover the complete postglacial sea history of the Baltic in these calculations. There are thus only five independent reference waters in the model, i.e. saline, preglacial altered, glacial melt, meteoric, and the three seawaters considered together (i.e. the Littorina Sea, postglacial altered water and the present Baltic Sea. See also Fig. 2-3).

In the study of the prototype repository near-field samples it was assumed that the six canisters did not affect the oxygen isotopic fractionation within the surrounding near-field water. This may well be a simplification. According to temperature measurements at the deposition hole–bedrock interface, the temperatures are high. At the end of 2004, the temperatures at the deposition hole interfaces were about 60–50°C (holes 1 and 3 in Section 1, and 5 and 6 in Section 2), although, the temperatures in the rock about 2 metres from the deposition holes were lower and varied from 40 to 50°C (Goudarzi & Johannesson 2005, 2006). For this reason, data from one sampled point (i.e. KA3572G01, not shown in Fig. 1-2) from Section 1 were not used in the inverse calculations because the location was between two heated canisters. Figure 1-2 shows that the sampling point KA3548G01 is also between heated canisters in Section 2. Heating in Section 2 began in May 2003, but it is not clear if the temperature is the reason for the isotopic changes in the samples from this location (cf. Fig. 3-2).

According to the results, the major source of water infiltrating the near field of the prototype repository is from above. The most significant individual source is the present Baltic Sea, the second largest source of water is the relict seawater reserves within the bedrock, and the third significant source of water is meteoric. Excavation for the Äspö HRL started in autumn 1990, and was essentially completed in the summer of 1995. The last samples considered in this study were collected at the beginning of 2004. Thus, the hydraulic gradients in the Äspö bedrock have been affected for almost ten years. However, there still seem to be significant relict water reserves above the major facilities of the HRL.

Table 3-5 summarises the approximate, cumulative mass transfer for each calculated near-field sample. The results indicate the extent of the chemical reactions that have occurred along the pathways from the water sources to the sampled locations. The results may be useful for forward modelling (on a similar regional scale), since gross values of reaction amounts are given. The approximate values of cumulative mass transfer given in Table 3-5 are based on measured values and interpretations i.e. attempts at forward modelling could be compared against these inverse interpretations. Successful calibration should provide a forward modelling tool with greater prediction reliability.

5 Acknowledgements

This work was financed by “in-kind” co-operation between Posiva and SKB, which is gratefully acknowledged. Sami Partamies from VTT helped with the practical work when it was most needed. Discussions with, and the comments of, Teresita Morales (SKB), Ignasi Puigdomenech (SKB), and Jukka-Pekka Salo (Posiva) were important for the completion of this work. The English language of this report was checked by Helen Sheppard (Word for Word).

6 References

Andersson, K., 1996. Mineralogy of the Äspö site. Swedish Nuclear Power Inspectorate (SKI), Stockholm. SKI Report 96:33. 10 p.

Andersson, J., Ahokas, H., Hudson, J.A., Koskinen, L., Luukkonen, A., Löfman, J., Keto, V., Pitkänen, P., Mattila, J., Ikonen, A.T.K. & Ylä-Mella, M., 2007. Olkiluoto site description 2006. Posiva Oy, Olkiluoto, Finland. Report POSIVA 2007-03. 536 p.

Appelo, C.A.J. & Postma, D., 1993. Geochemistry, groundwater and pollution. A.A. Balkema, Rotterdam. 536 p.

Appelo, C.A.J. & Postma, D., 2005. Geochemistry, groundwater and pollution. A.A. Balkema, Amsterdam, the Netherlands. 649 p.

Barcena, I. & Garcia-Sineriz, J.-L., 2001. Äspö Hard Rock Laboratory. Prototype Repository. System for canisters displacement tracking. Swedish Nuclear Fuel and Waste Management Co, Stockholm, Sweden. International Progress Report IPR-02-06. 27 p.

Börgesson, L. & Sandén, T., 2003. Äspö Hard Rock Laboratory. Prototype Repository. Instrumentation of buffer and backfill in Section II. Swedish Nuclear Fuel and Waste Management Co, Stockholm, Sweden. International Progress Report IPR-03-21. 55 p.

Canfield, D.E., Thamdrup, B. & Hansen, J.W., 1993. The anaerobic degradation of organic matter in Danish coastal sediments: Iron reduction, manganese reduction and sulfate reduction. Geochimica et Cosmochimica Acta 57, 3867–3883.

Desbarats, A.J. & Dirom, G.C., 2007. Temporal variations in the chemistry of circum-neutral drainage from the 10-level portal, Myra Mine, Vancouver Island, British Columbia. Applied Geochemistry 22, 415–435.

Eary, L.E., Runnells, D.D. & Esposito, K.J., 2003. Geochemical controls on ground water composition at the Cripple Creek Mining District, Cripple Creek, Colorado. Applied Geochemistry 18, 1–24.

Goudarzi, R. & Johannesson, L.-E., 2005. Äspö Hard Rock Laboratory. Prototype Repository. Sensors data report (Period 010917–051201). Report No: 14. Swedish Nuclear Fuel and Waste Management Co, Stockholm, Sweden. International Progress Report IPR-06-08. 441 p.

Goudarzi, R. & Johannesson, L.-E., 2006. Äspö Hard Rock Laboratory. Prototype Repository. Sensors data report (Period 010917–060601). Report No: 15. Swedish Nuclear Fuel and Waste Management Co, Stockholm, Sweden. International Progress Report IPR-06-26. 439 p.

Kankainen, T., 1986. Loviisa power station, final disposal of reactor waste. On the age and origin of groundwater from the rapakivi granite on the island of Hästholmen. Nuclear Waste Commission of Finnish Power Companies, Helsinki. Report YJT-86-29. 56 p.

Laaksoharju, M., 1988. Shallow groundwater chemistry at Laxemar, Äspö and Ävrö. Swedish Nuclear Fuel and Waste Management Co. (SKB), Stockholm. Progress Report 25-88-04. 15 p.

Laaksoharju, M. & Wallin, B. (eds.), 1997. Evolution of the groundwater chemistry at the Äspö Hard Rock Laboratory. Proceedings of the second Äspö International Geochemistry Workshop, June 6-7, 1995. Swedish Nuclear Fuel and Waste Management Co. (SKB), Stockholm. International Cooperation Report 97-04.

Luukkonen, A., 2006. Estimations of durability of fracture mineral buffers in the Olkiluoto bedrock. Posiva Oy, Olkiluoto, Finland. Working Report 2006-107. 38 p.

Luukkonen, A. & Kattilakoski, E., 2001. Äspö Hard Rock Laboratory. Groundwater flow, mixing and geochemical reactions at Äspö HRL. Task 5. Äspö Task Force on groundwater flow and transport of solutes. Swedish Nuclear Fuel and Waste Management Co. (SKB), Stockholm. International Progress Report IPR-02-41.

Parkhurst, D.L., 1997. Geochemical mole-balance modeling with uncertain data. Water Resources Research 33, 1957-1970.

Parkhurst, D.L. & Appelo, C.A.J., 1999. User's guide to PHREEQC (Version 2) – A computer program for speciation, batch-reaction, one dimensional transport, and inverse geochemical calculations. U.S. Geological Survey, Denver. Water-Resources Investigations Report 99-4259. 312 p.

Parkhurst, D.L. & Plummer, L.N., 1993. Geochemical models. In: (ed. Allen, W.M.) Regional ground-water quality. Van Nostrand Reinhold, New York, 199–225.

Plummer, L.N., Parkhurst, D.L. & Thorstenson, D.C., 1983. Development of reaction models for ground-water systems. Geochimica et Cosmochimica Acta 47, 665–686.

Pitkänen, P., Luukkonen, A., Ruotsalainen, P., Leino-Forsman, H. & Vuorinen, U., 1999. Geochemical modelling of groundwater evolution and residence time at the Olkiluoto site. Posiva Oy, Helsinki. Report POSIVA 98-10. 184 p.

Pitkänen, P., Partamies, S. & Luukkonen, A., 2004. Hydrogeochemical interpretation of baseline groundwater conditions at the Olkiluoto site. Posiva Oy, Olkiluoto, Finland. Report POSIVA 2003-07. 160 p.

Pusch, R. & Börgesson, L., 2001. Äspö Hard Rock Laboratory. Prototype Repository. Instrumentation of buffer and backfill in Section I. Swedish Nuclear Fuel and Waste Management Co, Stockholm, Sweden. International Progress Report IPR-01-60. 28 p.

Rhén, I., Forsmark, T. & Torin, L. (2001) Äspö Hard Rock Laboratory. Prototype Repository. Hydrogeological, hydrochemical and temperature measurements in boreholes during the operation phase of the Prototype Repository. Tunnel Section I. Swedish Nuclear Fuel and Waste Management Co, Stockholm, Sweden. International Progress Report IPR-01-32. 38 p.

Rhén, I., Forsmark, T., Magnusson, J. & Alm, P. (2003) Äspö Hard Rock Laboratory. Prototype Repository. Hydrogeological, hydrochemical, hydromechanical and temperature measurements in boreholes during the operation phase of the Prototype Repository. Tunnel Section II. Swedish Nuclear Fuel and Waste Management Co, Stockholm, Sweden. International Progress Report IPR-03-22. 65 p.

Puigdomenech, I. & Sandén, T., 2001. Äspö Hard Rock Laboratory. Prototype Repository. Instrumentation for gas and water sampling in buffer and backfill. Tunnel Section I. Swedish Nuclear Fuel and Waste Management Co, Stockholm, Sweden. International Progress Report IPR-01-62. 13 p.

Runnells, D.D., 1993. Inorganic chemical processes and reactions. In: (ed. Allen, W.M.) Regional ground-water quality. Van Nostrand Reinhold, New York. 131–153.

SKB, 2005. Äspö Hard Rock Laboratory. Annual Report 2004. Swedish Nuclear Fuel and Waste Management Co, Stockholm, Sweden. Technical Report TR-05-10. 211 p.

SKB, 2006. Geosphere process report for the safety assessment SR-Can. Swedish Nuclear Fuel and Waste Management Co. (SKB), Stockholm. Technical Report TR-06-19. 243 p.

SKB 2007. Äspö Hard Rock Laboratory. Annual report 2006. Swedish Nuclear Fuel and Waste Management Co. (SKB), Stockholm. Technical Report TR-07-10. 180 p.

Wang, Y. & Van Cappellen, P., 1996. A multicomponent reactive transport model of early diagenesis: Application to redox cycling in coastal marine sediments. Geochimica et Cosmochimica Acta 60, 2993–3014.

Appendices

Appendix 1. Summary of mass-transfer results for the baseline samples. The upper parts of the tables show mixing fractions of initial water samples for each final water sample. All values of mass transfer are expressed in mmol/L. A negative value indicates precipitation/cation uptake and a positive value dissolution/cation release. The minimum and maximum fractions and mass transfer possible within given analytical uncertainties are given after the representative values. (The results of the chemical analysis of each sample are presented in Appendix 3.)

Appendix 2. Summary of mass-transfer results for several prototype repository near-field samples. The upper parts of the tables give mixing fractions of initial water samples for each near-field water sample. Values of mass transfer are expressed in mmol/L. A negative value indicates precipitation/cation uptake and a positive value dissolution/cation release. The minimum and maximum fractions and mole transfer possible within given analytical uncertainties are given after the representative values. (The results of chemical analysis of each sample are presented in Appendix 4.)

Appendix 3. Results of chemical analysis of baseline samples from Äspö. Sampling was performed before excavations for the Äspö HRL. The complete analytical results have been saved in the SICADA database owned by SKB. Values denoted in boldface italics are estimates only. Secup and Seclow define upper and lower limits of sampling intervals and are given in metres along borehole. Northing, Easting, and Elevation give the mid-point of sampling locations and refer to the Swedish coordinate system.

Appendix 4. Results of chemical analysis of near-field water samples from the prototype repository. Sampling was carried out during construction and after the start of repository operation. The complete analytical results have been saved in the SICADA database owned by SKB. Secup and Seclow define upper and lower limits of sampling intervals and are given in metres along borehole. Northing, Easting, and Elevation give the mid-point of sampling locations and refer to the Swedish coordinate system.

Appendix 1 (1/3)

Sample	HAS06/-65.13			HAS07/-75.1			KAS06/-200.1			KAS06/-284.4			KAS03/-454.3		
Mixing fractions		min	max		min	max		min	max		min	max		min	max
Meteoric	**0.48**	0.47	0.49	**0.47**	0.41	0.57									
Baltic Sea	**0.30**	0.30	0.31												
Postglacial alt.															
Litorina Sea															
Glacial melt															
Preglacial alt.															
Saline															
HAS06/-65.1															
HAS07/-75.1							**0.53**	0.45	0.58						
KAS06/-200.1	**0.22**	0.20	0.23												
KAS06/-284.4							**0.23**	0.10	0.40						
KAS03/-454.3										**0.19**	0.19	0.24			
KAS04/-376.8							**0.24**	0.05	0.44						
KAS03/-121.8				**0.34**	0.23	0.38							**0.33**	0.27	0.36
KAS03/-239.0															
KAS03/-348.6															
KAS06/-433.3															
KAS06/-331.9				**0.19**	0.17	0.24				**0.81**	0.76	0.81			
KAS03/-602.5													**0.67**	0.64	0.73
KAS03/-830.1															
Mass transfer															
Calcite	**-1.11**	-	-0.86	**-2.69**	-4.75	-1.66	**-1.18**	-2.26	-0.23	**-1.30**	-	-0.64	**-0.63**	-0.98	-0.31
Dolomite	**0.00**	0.00	-	**0.34**	0.00	0.59	**0.00**	0.00	0.54	**0.00**	0.00	-	**0.00**	0.00	0.49
"CH_2O"	**0.00**	0.00	0.10	**0.29**	0.21	1.48	**1.49**	0.52	2.72	**1.16**	0.61	1.72	**0.62**	0.01	0.92
NaX	**0.00**	0.00	0.00	**-2.69**	-4.92	-0.27	**0.00**	0.00	0.00	**0.00**	0.00	0.00	**0.00**	0.00	0.00
KX	**-0.35**	-0.42	-0.28	**0.00**	0.00	0.00	**0.00**	0.00	0.00	**-0.04**	-0.07	0.00	**0.03**	0.01	0.05
CaX_2	**2.25**	2.01	-	**2.49**	1.08	4.50	**0.00**	0.00	0.00	**1.48**	0.92	-	**0.00**	0.00	0.00
MgX_2	**-1.49**	-	-1.27	**0.00**	0.00	0.00	**0.62**	0.10	1.14	**-0.73**	-	-0.46	**0.31**	-0.04	0.45
Goethite	**0.61**	0.46	0.84	**1.16**	0.85	2.36	**0.97**	0.23	1.78	**0.98**	0.49	1.39	**0.48**	0.00	0.69
FeX_2	**-0.58**	-0.81	-0.41	**-1.15**	-2.15	-0.83	**-0.62**	-1.14	-0.10	**-0.73**	-1.03	-0.36	**-0.33**	-0.48	0.02
Pyrite	**0.04**	0.03	0.06	**0.00**	-0.26	0.00	**-0.36**	-0.65	-0.13	**-0.26**	-0.39	-0.14	**-0.14**	-0.21	0.00

Appendix 1 (2/3)

Sample	KAS04/-376.8			KAS03/-121.8			KAS03/-239.0			KAS03/-348.6			KAS06/-433.3		
Mixing fractions		min	max		min	max		min	max		min	max		min	max
Meteoric															
Baltic Sea															
Postglacial alt.													**0.51**	0.43	0.57
Litorina Sea													**0.20**	0.14	0.24
Glacial melt				**0.67**	0.65	0.67	**0.36**	0.31	0.37						
Preglacial alt.				**0.33**	0.33	0.35	**0.24**	0.18	0.33						
Saline															
HAS06/-65.1															
HAS07/-75.1															
KAS06/-200.1															
KAS06/-284.4	**0.27**	0.25	0.31												
KAS03/-454.3															
KAS04/-376.8															
KAS03/-121.8										**0.36**	0.32	0.43			
KAS03/-239.0															
KAS03/-348.6							**0.40**	0.32	0.45						
KAS06/-433.3															
KAS06/-331.9										**0.16**	0.05	0.22			
KAS03/-602.5	**0.73**	0.69	0.75												
KAS03/-830.1										**0.47**	0.39	0.59	**0.29**	0.25	0.34
Mass transfer															
Calcite	**0.00**	0.00	0.00	**-0.11**	-	-0.01	**-4.48**	-5.47	-3.03	**-1.93**	-	-0.65	**-0.77**	-	-0.51
Dolomite	**0.00**	0.00	0.01	**0.00**	0.00	-	**0.63**	0.21	0.99	**0.00**	0.00	-	**0.00**	0.00	-
"CH_2O"	**0.00**	0.00	0.04	**0.02**	0.00	0.23	**3.20**	2.41	3.62	**1.51**	0.05	2.61	**0.11**	0.07	2.28
NaX	**0.00**	0.00	0.00	**0.00**	0.00	0.00	**3.37**	2.67	4.02	**3.26**	2.28	-	**0.00**	0.00	0.00
KX	**0.00**	0.00	0.00	**0.06**	0.05	0.06	**0.10**	0.08	0.13	**0.00**	0.00	0.00	**-0.89**	-1.11	-0.65
CaX_2	**0.00**	0.00	0.00	**0.70**	0.54	-	**0.00**	0.00	0.00	**0.00**	0.00	0.00	**4.45**	3.02	-
MgX_2	**0.01**	-0.01	0.01	**-0.65**	-	-0.55	**0.00**	0.00	0.00	**-0.57**	-	-0.35	**-3.53**	-	-2.30
Goethite	**0.01**	0.00	0.02	**0.08**	0.01	0.32	**2.47**	1.94	2.88	**1.39**	0.21	2.20	**0.46**	0.29	2.11
FeX_2	**-0.01**	-0.01	0.01	**-0.09**	-0.29	-0.02	**-1.74**	-2.05	-1.40	**-1.06**	-1.61	-0.21	**-0.47**	-1.62	-0.29
Pyrite	**0.00**	-0.01	0.00	**0.00**	-0.04	0.00	**-0.74**	-0.84	-0.54	**-0.33**	-0.59	0.00	**0.00**	-0.50	0.00

Appendix 1 (3/3)

Sample	KAS06/-331.9			KAS03/-602.5			KAS03/-830.1		
Mixing fractions		min	max		min	max		min	max
Meteoric									
Baltic Sea									
Postglacial alt.	**0.40**	0.40	0.40						
Litorina Sea							**0.09**	0.05	0.14
Glacial melt									
Preglacial alt.									
Saline							**0.58**	0.52	0.62
HAS06/-65.1									
HAS07/-75.1									
KAS06/-200.1									
KAS06/-284.4									
KAS03/-454.3									
KAS04/-376.8									
KAS03/-121.8							**0.33**	0.32	0.34
KAS03/-239.0				**0.39**	0.38	0.41			
KAS03/-348.6									
KAS06/-433.3	**0.60**	0.60	0.60						
KAS06/-331.9									
KAS03/-602.5									
KAS03/-830.1				**0.61**	0.59	0.62			
Mass transfer									
Calcite	**-0.37**	-0.72	-0.25	**-0.32**	-	-0.28	**-0.35**	-	-0.30
Dolomite	**0.00**	0.00	0.01	**0.00**	0.00	-	**0.00**	0.00	-
"CH_2O"	**0.06**	0.03	0.29	**0.05**	0.04	0.49	**0.05**	0.04	0.20
NaX	**0.00**	0.00	0.00	**0.00**	0.00	0.00	**0.00**	0.00	0.00
KX	**-0.21**	-0.26	-0.16	**0.00**	0.00	0.00	**-0.27**	-0.48	-0.13
CaX_2	**0.34**	0.23	0.57	**0.69**	0.52	-	**1.64**	0.78	-
MgX_2	**0.00**	0.00	0.00	**-0.50**	-	-0.35	**-1.30**	-	-0.54
Goethite	**0.22**	0.14	0.48	**0.19**	0.16	0.54	**0.20**	0.17	0.35
FeX_2	**-0.24**	-0.44	-0.15	**-0.19**	-0.44	-0.17	**-0.21**	-0.32	-0.17
Pyrite	**0.00**	-0.05	0.00	**0.00**	-0.10	0.00	**0.00**	-0.03	0.00

Appendix 2 (1/3)

Sample	KA3539G Aug. 2, 1998			KA3539G May 23, 2003			KA3539G Sept. 24, 2003			KA3539G Feb. 16, 2004			KA3542G01 July 31, 1998		
		min	max		min	max		min	max		min	max		min	max
Mixing fractions															
HAS07/-75.1	**0.22**	0.17	0.30	**0.28**	0.20	0.33									
HAS06/-65.1													**0.37**	0.23	0.48
Baltic Sea	**0.52**	0.39	0.60	**0.46**	0.38	0.53	**0.49**	0.41	0.53	**0.50**	0.45	0.54	**0.34**	0.16	0.51
KAS06/-331.9	**0.26**	0.23	0.31										**0.29**	0.23	0.36
KAS06/-200.1							**0.39**	0.32	0.54	**0.42**	0.34	0.51			
KAS06/-284.4				**0.26**	0.20	0.32	**0.12**	0.00	0.21	**0.08**	0.00	0.18			
Mass transfer															
Calcite															
Dolomite	**0.16**	0.00	0.20	**0.10**	0.00	0.13	**0.00**	0.00	0.17	**0.12**	0.00	0.15	**0.13**	0.00	0.18
"CH_2O"	**1.26**	1.09	1.78	**0.89**	0.73	1.30	**1.11**	0.65	1.32	**0.73**	0.56	1.01	**0.82**	0.58	1.41
NaX															
KX	**-0.84**	-1.06	-0.57	**-0.73**	-0.93	-0.54	**-0.75**	-0.90	-0.56	**-0.79**	-0.94	-0.64	**-0.60**	-0.94	-0.28
CaX_2	**3.94**	2.73	4.96	**3.48**	2.64	4.35	**3.88**	3.04	4.50	**3.81**	3.20	4.48	**3.06**	1.62	4.55
MgX_2	**-3.87**	-4.77	-2.74	**-3.36**	-4.12	-2.57	**-3.60**	-4.27	-2.97	**-3.63**	-4.21	-3.06	**-2.96**	-4.30	-1.61
Goethite	**0.00**	0.00	0.30	**0.00**	0.00	0.21	**0.21**	0.00	0.26	**0.00**	0.00	0.20	**0.00**	0.00	0.28
FeX_2	**0.36**	0.14	0.41	**0.25**	0.10	0.30	**0.09**	0.06	0.29	**0.21**	0.05	0.26	**0.20**	0.01	0.29
Pyrite	**-0.36**	-0.49	-0.31	**-0.25**	-0.36	-0.21	**-0.30**	-0.36	-0.18	**-0.21**	-0.27	-0.16	**-0.23**	-0.39	-0.17

Sample	KA3542G01 June 2, 2003			KA3542G01 Sept.24,2003			KA3542G01 Nov. 9, 2004			KA3548A01 Aug. 6, 1998			KA3548A01 June 2, 2003		
		min	max		min	max		min	max		min	max		min	max
Mixing fractions															
HAS07/-75.1	**0.31**	0.22	0.40										**0.35**	0.26	0.43
HAS06/-65.1										**0.33**	0.26	0.44			
Baltic Sea	**0.54**	0.43	0.64	**0.48**	0.38	0.53	**0.40**	0.35	0.46	**0.44**	0.27	0.55	**0.50**	0.37	0.62
KAS06/-331.9										**0.22**	0.19	0.29	**0.15**	0.10	0.21
KAS06/-200.1				**0.33**	0.24	0.49	**0.40**	0.30	0.49						
KAS06/-284.4	**0.15**	0.10	0.20	**0.19**	0.06	0.30	**0.20**	0.11	0.31						
Mass transfer															
Calcite															
Dolomite	**0.19**	0.00	0.22	**0.09**	0.00	0.12	**0.04**	0.00	0.07	**0.00**	0.00	0.20	**0.22**	0.00	0.25
"CH_2O"	**1.17**	0.99	1.77	**0.68**	0.49	1.07	**0.35**	0.20	0.63	**1.42**	0.87	1.69	**1.20**	1.02	1.84
NaX															
KX	**-0.84**	-1.10	-0.59	**-0.71**	-0.87	-0.49	**-0.62**	-0.78	-0.47	**-0.78**	-1.03	-0.45	**-0.78**	-1.07	-0.51
CaX_2	**3.49**	2.39	4.68	**3.33**	2.39	4.04	**3.63**	3.03	4.33	**3.30**	1.82	4.46	**3.42**	2.24	4.67
MgX_2	**-3.40**	-4.45	-2.30	**-3.19**	-3.81	-2.33	**-3.44**	-4.03	-2.89	**-3.04**	-4.17	-1.73	**-3.37**	-4.48	-2.26
Goethite	**0.00**	0.00	0.35	**0.00**	0.00	0.19	**0.00**	0.00	0.11	**0.24**	0.00	0.30	**0.00**	0.00	0.39
FeX_2	**0.33**	0.09	0.38	**0.21**	0.08	0.27	**0.11**	0.04	0.16	**0.13**	0.07	0.36	**0.34**	0.07	0.39
Pyrite	**-0.33**	-0.48	-0.28	**-0.19**	-0.29	-0.14	**-0.10**	-0.17	-0.06	**-0.39**	-0.46	-0.25	**-0.34**	-0.50	-0.29

Appendix 2 (2/3)

Sample	KA3548A01 Sept.24,2003			KA3548A01 Feb.16,2004			KA3554G01 June 3, 2003			KA3554G01 Sept.24,2003			KA3554G01 Mar. 2, 2004		
		min	max		min	max		min	max		min	max		min	max
Mixing fractions															
HAS07/-75.1							**0.33**	0.28	0.42						
HAS06/-65.1													**0.30**	0.15	0.40
Baltic Sea	**0.44**	0.38	0.47	**0.36**	0.31	0.38	**0.61**	0.50	0.71	**0.46**	0.40	0.51	**0.37**	0.24	0.51
KAS06/-331.9							**0.06**	0.01	0.10						
KAS06/-200.1	**0.32**	0.26	0.43	**0.31**	0.24	0.34				**0.36**	0.27	0.47			
KAS06/-284.4	**0.24**	0.13	0.33	**0.34**	0.29	0.44				**0.18**	0.07	0.29	**0.33**	0.27	0.40
Mass transfer															
Calcite															
Dolomite	**0.09**	0.00	0.12	**0.07**	0.00	0.09	**0.00**	0.00	0.35	**0.12**	0.00	0.15	**0.11**	0.00	0.16
"CH_2O"	**0.66**	0.49	0.82	**0.54**	0.41	0.58	**2.23**	1.41	2.45	**0.83**	0.65	1.17	**0.85**	0.60	1.41
NaX															
KX	**-0.65**	-0.78	-0.49	**-0.55**	-0.64	-0.41	**-0.93**	-1.19	-0.66	**-0.67**	-0.83	-0.51	**-0.61**	-0.90	-0.33
CaX_2	**3.31**	2.64	3.85	**3.31**	2.79	3.79	**3.62**	2.39	4.67	**3.41**	2.75	4.10	**3.03**	1.71	4.52
MgX_2	**-3.17**	-3.64	-2.56	**-3.20**	-3.60	-2.72	**-3.27**	-4.51	-2.22	**-3.32**	-3.91	-2.71	**-2.94**	-4.33	-1.68
Goethite	**0.00**	0.00	0.15	**0.00**	0.00	0.10	**0.48**	0.00	0.53	**0.00**	0.00	0.22	**0.00**	0.00	0.25
FeX_2	**0.19**	0.06	0.23	**0.16**	0.05	0.16	**0.12**	0.09	0.51	**0.24**	0.08	0.29	**0.22**	0.05	0.31
Pyrite	**-0.19**	-0.22	-0.14	**-0.15**	-0.16	-0.12	**-0.60**	-0.66	-0.40	**-0.24**	-0.32	-0.19	**-0.24**	-0.39	-0.17

Sample	KA3554G02 July 21,1998			KA3554G02 June30,2003			KA3554G02 Nov. 19, 2004			KA3566G02 Apr. 8, 1999			KA3566G02 June 4, 2003		
		min	max		min	max		min	max		min	max		min	max
Mixing fractions															
HAS07/-75.1															
HAS06/-65.1	**0.31**	0.18	0.42												
Baltic Sea	**0.48**	0.35	0.67	**0.49**	0.40	0.53	**0.37**	0.36	0.37	**0.56**	0.45	0.66	**0.56**	0.52	0.64
KAS06/-331.9	**0.21**	0.15	0.27							**0.21**	0.11	0.33			
KAS06/-200.1				**0.43**	0.34	0.49	**0.38**	0.37	0.38	**0.23**	0.11	0.33	**0.44**	0.36	0.48
KAS06/-284.4				**0.08**	0.04	0.18	**0.25**	0.25	0.26						
Mass transfer															
Calcite							**-1.53**	-	-0.87						
Dolomite	**0.00**	0.00	0.23	**0.09**	0.00	0.13				**0.00**	0.00	0.20	**0.00**	0.00	0.21
"CH_2O"	**1.82**	1.17	2.16	**0.60**	0.46	1.00	**1.80**	1.07	1.85	**1.82**	1.29	2.05	**1.27**	0.77	1.44
NaX															
KX	**-0.81**	-1.20	-0.53	**-0.78**	-0.92	-0.56	**-0.56**	-0.62	-0.48	**-0.90**	-1.16	-0.65	**-0.88**	-1.09	-0.73
CaX_2	**3.07**	1.80	4.80	**3.75**	2.78	4.42	**3.98**	3.36	-	**3.51**	2.34	4.60	**3.85**	3.12	4.83
MgX_2	**-2.86**	-4.53	-1.78	**-3.53**	-4.12	-2.59	**-2.90**	-	-2.64	**-3.30**	-4.29	-2.30	**-3.48**	-4.51	-2.84
Goethite	**0.27**	0.00	0.36	**0.00**	0.00	0.20	**1.23**	0.71	1.34	**0.26**	0.00	0.32	**0.28**	0.00	0.32
FeX_2	**0.20**	0.13	0.48	**0.17**	0.04	0.22	**-0.80**	-0.91	-0.42	**0.25**	0.20	0.48	**0.06**	0.04	0.30
Pyrite	**-0.50**	-0.60	-0.34	**-0.17**	-0.27	-0.13	**-0.43**	-0.43	-0.25	**-0.50**	-0.56	-0.37	**-0.34**	-0.39	-0.22

Appendix 2 (3/3)

Sample	KA3566G02 Sept.29,2003			KA3590G01 Sept.30,2003			KA3590G01 Mar. 4, 2004			KG0021A01 Dec. 9, 1998			KG0021A01 June30,2003		
		min	max		min	max		min	max		min	max		min	max
Mixing fractions															
HAS07/-75.1				**0.30**	0.20	0.39	**0.33**	0.25	0.42						
HAS06/-65.1										**0.33**	0.25	0.44	**0.32**	0.22	0.44
Baltic Sea	**0.51**	0.50	0.58	**0.56**	0.45	0.66	**0.55**	0.46	0.65	**0.52**	0.36	0.65	**0.51**	0.38	0.61
KAS06/-331.9										**0.15**	0.11	0.21			
KAS06/-200.1	**0.49**	0.42	0.50										**0.17**	0.08	0.26
KAS06/-284.4				**0.15**	0.10	0.20	**0.13**	0.08	0.18						
Mass transfer															
Calcite															
Dolomite	**0.13**	0.00	0.16	**0.23**	0.00	0.27	**0.25**	0.00	0.28	**0.00**	0.00	0.25	**0.00**	0.00	0.28
"CH_2O"	**0.82**	0.68	1.25	**1.41**	1.22	2.11	**1.50**	1.30	2.21	**1.71**	1.04	2.00	**1.93**	1.18	2.24
NaX															
KX	**-0.75**	-0.96	-0.67	**-0.83**	-1.10	-0.58	**-0.82**	-1.09	-0.61	**-0.90**	-1.20	-0.59	**-0.81**	-1.06	-0.54
CaX_2	**3.35**	2.88	4.30	**3.54**	2.41	4.74	**3.31**	2.39	4.51	**3.40**	1.95	4.71	**2.69**	1.32	3.86
MgX_2	**-3.20**	-4.06	-2.67	**-3.52**	-4.58	-2.34	**-3.33**	-4.38	-2.44	**-3.07**	-4.31	-1.81	**-2.44**	-3.68	-1.23
Goethite	**0.00**	0.00	0.24	**0.00**	0.00	0.42	**0.00**	0.00	0.44	**0.32**	0.00	0.39	**0.35**	0.00	0.43
FeX_2	**0.23**	0.06	0.27	**0.40**	0.11	0.46	**0.43**	0.12	0.48	**0.12**	0.06	0.41	**0.15**	0.09	0.47
Pyrite	**-0.23**	-0.34	-0.20	**-0.40**	-0.58	-0.35	**-0.43**	-0.60	-0.37	**-0.47**	-0.55	-0.30	**-0.52**	-0.61	-0.34

Sample	KG0021A01 Sept.18,2003			KG0021A01 Feb.17,2004			KG0048A01 June 3, 2003			KG0048A01 Sept.18,2003			KG0048A01 Mar. 2, 2004		
		min	max		min	max		min	max		min	max		min	max
Mixing fractions															
HAS07/-75.1	**0.30**	0.21	0.35	**0.31**	0.22	0.36	**0.34**	0.26	0.40	**0.23**	0.19	0.29	**0.29**	0.20	0.36
HAS06/-65.1															
Baltic Sea	**0.55**	0.46	0.64	**0.50**	0.43	0.58	**0.66**	0.60	0.74	**0.54**	0.43	0.57	**0.48**	0.42	0.57
KAS06/-331.9															
KAS06/-200.1															
KAS06/-284.4	**0.14**	0.10	0.20	**0.19**	0.14	0.25				**0.23**	0.18	0.29	**0.23**	0.18	0.29
Mass transfer															
Calcite															
Dolomite	**0.21**	0.00	0.25	**0.18**	0.00	0.22	**0.28**	0.00	0.32	**0.18**	0.00	0.22	**0.18**	0.00	0.22
"CH_2O"	**1.46**	1.27	2.13	**1.17**	1.00	1.76	**1.74**	1.54	2.54	**1.25**	1.07	1.83	**1.20**	1.02	1.79
NaX							**-2.96**	-5.66	-0.59						
KX	**-0.79**	-1.04	-0.57	**-0.74**	-0.96	-0.55	**-0.97**	-1.22	-0.78	**-0.76**	-0.88	-0.49	**-0.70**	-0.93	-0.53
CaX_2	**2.63**	1.62	3.76	**2.82**	2.00	3.81	**4.74**	3.78	6.09	**2.78**	1.60	3.34	**3.00**	2.32	4.07
MgX_2	**-2.65**	-3.63	-1.65	**-2.78**	-3.65	-2.00	**-3.27**	-4.36	-2.32	**-2.77**	-3.24	-1.64	**-2.99**	-3.93	-2.33
Goethite	**0.00**	0.00	0.39	**0.00**	0.00	0.34	**0.00**	0.00	0.50	**0.00**	0.00	0.34	**0.00**	0.00	0.34
FeX_2	**0.41**	0.14	0.47	**0.33**	0.10	0.39	**0.49**	0.15	0.55	**0.36**	0.12	0.41	**0.34**	0.11	0.40
Pyrite	**-0.42**	-0.58	-0.36	**-0.33**	-0.48	-0.29	**-0.50**	-0.69	-0.44	**-0.36**	-0.50	-0.30	**-0.34**	-0.49	-0.29

Appendix 3

Idcode	Secup (m)	Seclow (m)	Sample #	Date	Northing (m)	Easting (m)	Elevation (m)	Na mg/l	K mg/l	Ca mg/l	Mg mg/l	HCO_3 mg/l	Cl mg/l	SO_4 mg/l	Fetot mg/l	pH pH unit	$\delta^{18}O$ ‰SMOW
HAS06/-65.1	40	100	2	Aug. 8, 1987	6367992.09	1551592.57	-65.134	900	12.0	297	56.0	155	1760	283.0	4.70	7.8	-9.4
HAS07/-75.1	71	100	1	Aug. 2, 1987	6368153.89	1551563.32	-75.049	669	5.0	347	48.0	102	1650	122.0	1.40	7.7	-11.2
KAS03/-121.8	129	134	1569	Feb. 21, 1989	6368227.89	1550996.93	-121.810	613	2.4	162	21.0	61	1220	31.1	0.13	8.0	-15.8
KAS03/-239.0	248	251	1448	Aug. 28, 1988	6368239.80	1550989.20	-238.951	1290	6.5	490	58.0	53	2950	39.0	***0.30***	7.8	-14.5
KAS03/-348.6	347	373	1441	Aug. 16, 1988	6368251.94	1550982.77	-348.592	1770	5.9	1400	40.0	12	5180	370.0	***0.10***	***7.5***	-13.3
KAS03/-454.3	453	480	1445	Aug. 22, 1988	6368263.53	1550976.56	-454.275	1550	6.2	1190	40.0	27	4600	300.0	***0.50***	7.8	-13.6
KAS03/-602.5	609	623	1452	Sept. 3, 1988	6368280.57	1550966.71	-602.474	1920	6.2	1740	38.0	11	5880	470.0	***0.10***	8.1	-13.3
KAS03/-830.1	690	1002.1	1455	Sept. 8, 1988	6368310.50	1550951.76	-830.051	2130	6.6	2670	45.0	11	8080	680.0	0.05	8.0	-13.0
KAS04/-376.8	440	480.98	1588	Mar. 3, 1989	6367941.95	1551340.14	-376.789	1890	7.8	1660	61.0	21	5840	407.0	0.26	8.1	-11.9
KAS06/-200.1	204	277	1606	June 31, 1989	6367740.57	1551504.94	-200.067	1230	7.4	893	82.0	89	3630	150.0	0.44	7.6	-10.9
KAS06/-284.4	304	377	1610	June 7, 1989	6367794.28	1551506.51	-284.403	1820	9.1	1490	119.0	49	5680	283.0	0.43	7.5	-9.2
KAS06/-331.9	389	406	1614	June 14, 1989	6367825.77	1551508.34	-331.873	2070	11.7	1410	153.0	64	5970	362.0	0.85	7.3	-7.4
KAS06/-433.3	439	602.17	1618	June 21, 1989	6367895.41	1551512.44	-433.277	2200	11.1	1570	130.0	50	6150	459.0	0.63	7.3	-8.2

Appendix 4

Idcode	Secup (m)	Seclow (m)	Sample #	Date	Northing (m)	Easting (m)	Elevation (m)	Na mg/l	K mg/l	Ca mg/l	Mg mg/l	HCO_3 mg/l	Cl mg/l	SO_4 mg/l	Fe-ICP mg/l	pH pH unit	$\delta^{18}O$ ‰SMOW
Measurement uncertainty:								4%	6%	4%	4%	4%	5%	6%	5%	0.02 unit	0.2 unit
KA3539G	15	18	2594	Aug. 2, 1998	6367761.38	1551222.89	-463.956	1610	9.2	643	77.7	180	3840	322	0.27	7.3	-7.7
KA3539G	15.85	17.6	6039	June 23, 2003	6367761.37	1551222.75	-464.794	1570	8.94	666	70	147	3700	316	0.22	7.3	-8.6
KA3539G	15.85	17.6	6201	Sept. 24, 2003	6367761.37	1551222.75	-464.794	1650	10.3	727	69.8	150	3770	316	0.22	7.5	-8.8
KA3539G	15.85	17.6	6264	Feb. 16, 2004	6367761.37	1551222.75	-464.794	1600	9.18	702	71.4	142	3810	334	0.23	7.5	-8.8
KA3542G01	18	21	2590	July 31, 1998	6367748.05	1551222.33	-461.764	1610	9.2	678	73.8	170	3940	355	0.25	7.5	-7.8
KA3542G01	18.6	20.3	6041	June 2, 2003	6367747.63	1551222.35	-462.188	1520	9.44	528	76.2	179	3290	291	0.67	7.5	-8.3
KA3542G01	18.6	20.3	6200	Sept. 24, 2003	6367747.63	1551222.35	-462.188	1700	11.3	763	82.4	132	3960	325	1.33	7.4	-8.7
KA3542G01	18.6	20.3	6390	Nov. 9, 2004	6367747.63	1551222.35	-462.188	1660	10	835	65	106	4060	362	0.73	7.42	-9.0
KA3548A01	9	10	2596	Aug. 6, 1998	6367749.40	1551216.28	-477.037	1560	8.7	586	79.6	190	3620	299	0.29	7.4	-7.6
KA3548A01	8.8	10.75	6040	June 2, 2003	6367749.60	1551216.27	-477.026	1510	9.56	527	76.5	187	3270	289	0.21	7.6	-8.2
KA3548A01	8.8	10.75	6199	Sept. 24, 2003	6367749.60	1551216.27	-477.026	1730	11.3	817	79.3	129	4100	335	0.35	7.4	-8.9
KA3548A01	8.8	10.75	6263	Feb. 16, 2004	6367749.60	1551216.27	-477.026	1790	10.1	943	70.4	116	4220	360	0.30	7.4	-9.1
KA3554G01	22.6	24.15	6043	June 3, 2003	6367744.03	1551210.66	-464.796	1460	10.7	396	84.2	225	2980	259	0.25	7.7	-8.0
KA3554G01	22.6	24.15	6202	Sept. 24, 2003	6367744.03	1551210.66	-464.796	1680	11.6	774	77.3	145	3910	325	0.38	7.4	-8.8
KA3554G01	22.6	24.15	6274	Mar. 2, 2004	6367744.03	1551210.66	-464.796	1600	10.1	739	71.4	159	3750	326	0.42	7.4	-8.2
KA3554G02	11	12	2579	July 21, 1998	6367768.76	1551209.06	-456.569	1630	9.9	553	89.1	213	3790	299	0.37	7.3	-7.4
KA3554G02	10.5	12.2	6048	June 30, 2003	6367768.41	1551209.08	-456.215	1700	9.52	699	72.7	132	3930	303	0.11	7.5	-8.8
KA3554G02	10.5	12.2	6394	Nov. 19, 2004	6367768.41	1551209.08	-456.215	1760	10.3	782	70.7	94	3890	328	0.18	7.55	-9.2
KA3566G02	12.3	18.3	2880	Apr. 8, 1999	6367769.08	1551196.97	-457.054	1840	9.9	693	98	192	4110	277	0.23	7.2	-7.6
KA3566G02	16	18	6044	June 4, 2003	6367771.74	1551196.78	-459.615	1610	10.1	556	79	164	3610	279	0.11	7.7	-8.4
KA3566G02	16	18	6210	Sept. 29, 2003	6367771.74	1551196.78	-459.615	1700	11.2	650	80.3	153	3690	291	0.20	7.5	-8.6
KA3566G02	16	18	6393	Nov. 19, 2004	6367771.74	1551196.78	-459.615	2680	10.9	671	74.4	111	4220	347	0.14	7.51	-8.7
KA3590G01	15.2	23.5	6211	Sept. 30, 2003	6367746.87	1551174.68	-458.669	1530	11	522	78.1	199	3250	281	0.37	7.5	-8.2
KA3590G01	15.2	23.5	6265	March 4, 2004	6367746.87	1551174.68	-458.669	1480	10.5	494	79.5	207	3130	291	0.24	7.5	-8.3
KG0021A01	35	36	2685	Dec. 9, 1998	6367763.68	1551217.03	-434.503	1560	8.2	494	84	209	3420	295	0.03	7.5	-7.5
KG0021A01	35	36	6047	June 30, 2003	6367763.68	1551217.03	-434.503	1440	10.8	402	88.3	225	3000	268	0.22	7.5	-8.1
KG0021A01	35	36	6184	Sept. 18, 2003	6367763.68	1551217.03	-434.503	1590	12.2	483	97.4	200	3250	288	0.29	7.4	-8.3
KG0021A01	35	36	6267	Feb. 17, 2004	6367763.68	1551217.03	-434.503	1550	11.1	559	88.1	177	3490	308	0.28	7.47	-8.5
KG0048A01	32.8	33.8	6042	June 3, 2003	6367769.33	1551189.78	-436.523	1440	11.9	378	93.1	231	2980	270	0.33	7.5	-8.0
KG0048A01	32.8	33.8	6186	Sept. 18, 2003	6367769.33	1551189.78	-436.523	1660	13.4	585	98.3	179	3630	305	0.56	7.4	-8.5
KG0048A01	32.8	33.8	6275	Mar. 02, 2004	6367769.33	1551189.78	-436.523	1560	11.2	616	81.1	177	3480	309	0.24	7.44	-8.5